University of Stavanger

Faculty of Science and Technology

MASTER'S THESIS

Study program/ Specialization: **Petroleum technology/** **Reservoir engineering**	Spring semester, 2013 Restricted access
Writer: **Lieu Thuy Pham**	…… (Writer's signature)
Faculty supervisor: **Dimitrios G. Hatzignatiou** External supervisor(s): **Arne Stavland**	
Title of thesis: **Rheological Evaluation of a Sodium Silicate Gel for Water Management in Mature Oilfields**	
Credits (ECTS): 30	
Key words: Water Conformance Silicate gel Sodium Silicate Solution Rheological properties Sol-gel Transition Time Gel strength	Pages: 91 pages + enclosure: 2 CDs Stavanger, 17/6/2013

ACKNOWLEDGEMENTS

It would not have been possible to write this Masters' thesis without the help and support of the kind people around me, to only some of whom it is possible to give particular mention here.

First and foremost I offer my sincerest gratitude to my supervisor, Professor Dimitrios Georgios Hatzignatiou. This thesis would not have been possible without help, support and patience, not to mention his advices and unsurpassed knowledge. I attribute the level of my Masters' degree to his encouragement and effort: one simply could not wish for a better and friendlier supervisor.

The good advice, support and friendship of my second supervisor, Arne Stavland, has been invaluable on both an academic and a personal level, for which I am extremely grateful.

In my daily work I have been blessed with a friendly and cheerful group of fellow co-workers: Nils Harald Giske, Reza Askarinezhad and Kim André Nesse Vorland.

I would like to acknowledge the financial support of Talisman and the academic and technical support of the University of Stavanger and IRIS, along with their respective staff.

Finally, I thank Michel for his personal support and great patience at all times. My family has given me their unequivocal support throughout, as always, for which my mere expression of thanks likewise does not suffice.

TABLE OF CONTENTS

LIST OF FIGURES

Abstract

Excess water production is a common problem in mature and hydrocarbon rate declining oil and gas fields. Increased water production rates reduce oil and gas production, increase the cost related with fluid lifting, handling and disposal of produced water and negatively impacts the hydrocarbon production economics. Among the various techniques for water control, silicate gel system is known to be an effective and environmentally friendly method for water shutoff treatment. This gel system usually contents two main components, which are the liquid silica and activator. The system that has a low viscosity (almost like water) is mixed and pumped from surface in liquid form. The gelation time has been designed to be delayed under reservoir conditions thus allowing sufficient time for the pumped fluids to reach the designated distance from the treatment well. After certain time, a hard gel is formed that blocks high permeable zones and eliminate unwanted flow of water towards the production wells.

This thesis focuses on the laboratory qualification of a sodium silicate gel system for designing and implementing water shutoff treatments in the field. Lab rheology measurements were carried on sodium silicate gel samples using the Anton Paar Rheomter MCR302. Two test modes were run with the specific purposes: the Dynamic-Mechanical (DMA) mode is employed to determine the onset of the gelation (sol-gel transition time or gel point) and the viscosity increase versus time; the Amplitude sweep mode is used to assess the formed gel's shear strength at a given viscosity. Gel point and gel strength play an important role in designing successful water shutoff treatments since the first determines the required time for injecting the gelant system into the reservoir and other determines the force the formed gel can withstand under shear conditions.

The effects of silicate and activator concentrations, presence of divalent ions (e.g., Ca^{2+}, Mg^{2+}), temperature, and gelant dilution on sol-gel transition time were investigated. A general equation, which describes the relation between sol-gel transition times with all mentioned factors, was developed for field application's design later.

1 Introduction

Water flooding is the easiest and cost-effective mean for maintaining reservoir pressure and increasing oil production efficiency. However, due to high mobility of water compared to reservoir oil, most of the injected water flows through the high permeability zones, leaving large amounts of upswept oil in the reservoir. Subsequently, oil production rate is reduced while water production is increased over time, thus leading to excessive water production. Economic concerns are related not only with the large amounts of oil remaining in the reservoir, but also with the large time-increasing costs associated with the produced water in terms of lifting, processing, treating and reinjection and/or disposal. Therefore, improve oil recovery factors could be achieved by addressing the problem of excessive water production and its effective utilization to displace mobile reservoir oil. A typical water shutoff treatment could reduce water production by 75% to 90% and increase oil production by 1,000% (Portwood, 1999).

There are several mechanical and chemical methods that can be applied to reduce water production, both with near-well and in-depth treatments. An example of a mechanical near-well treatment is cement bridge plugs, which can be deployed to isolate the most productive layers. However, in reservoir where the different layers are in communication, this method will not affect the fractional flow because of fluid cross-flow (Skrettingland, et al., 2012). For this case, chemical in-depth treatments are more advantageous over the mechanical methods. Injected chemicals are designed to form gel in designated places, which can be fractures, high water permeability zones, thief zones, etc. Subsequently, the injected water is diverted into non-swept zones of the reservoir yielding increased oil recovery.

Polymers have been studied and used more than silicate for water-shutoff operation. However, these robust and effective chemical systems are currently listed either as black or red according to Norwegian environmental regulations and are therefore not being used in Norway (Bjørn, et al., 2011). Recent studies and field tests have demonstrated the feasibility and efficiency of silicate gel as water-control chemicals. Moreover, silicate is categorized as a green chemical and is more environmental friendly than most other chemicals used for diversion, which is one of the most preferable criteria for chemical usage in Norway (Stavland, et al., 2011).

As any other system, silicate gel systems have their own advantages and disadvantages. Recognizing these advantages, various studies have been performed to better understand the silicate gel systems' behavior and tested different additives to improve their performance (Vinot *et al.* (1989), Nasr-El-Din *et al.* (2005)).

In this work, a sodium silicate solution is studied as a means of addressing water production issues. The gelling system contains of 2 main components: commercial sodium silicate solution and activator. The mixture with the designed concentration of components is injected into formation and forms a rigid gel at the required time and at reservoir temperature. There are several factors that control the gelation time of the gel system, such as gelling agent (sodium silicate itself) and activator concentration, mixing water salinity and most importantly, temperature.

The main objectives of this thesis are to:

- Evaluate the effects of different factors on the sol-gel transition time.
- Derive a general equation that can be used to determine the sol-gel transition time.
- Assess the strength of the formed gel based on shear stress at specific viscosity of gel.

2 Literature Survey

In this section a thorough review of available books and scientific papers is presented. Firstly, the origins of water production are summarized. Secondly, an overview of possible impacts of excess water production is presented. And lastly, the different solutions to control water production correspond to each circumstance are examined and silicate gel system is highlighted as an effective method for water control.

2.1 Origins of water production

Formation water produced together with oil and gas is usually considered as an undesirable byproduct of hydrocarbon production. Besides the formation water, the injected water during water flooding or for pressure maintenance also contributes to the water content in the produced hydrocarbon/water fluid mixture at surface.

The water is considered as “good water” when it produces oil with it and at a rate below the WOR (water-oil ratio) economic limit. However, as the field becomes more depleted, the amount of produced water increases and at some point the WOR exceeds the economic limit. At this stage, the water is considered as “bad water” or excessive water (Bailey, et al., 2000)

There are numerous technologies developed to control the excessive water production, but the mechanism of its occurrence must be understood in order to design an effective treatment. In individual wells, the source of most excessive water production can be classified as one of ten basic types. The ten basic problem types vary from easy to the most difficult to solve (Bailey, et al., 2000):

- *Casing, tubing or packer leaks* – Leaks through casing, tubing or packers allow water from non-oil productive zones to enter the production string.
- *Channel flow behind casing* – Failed primary cementing can connect water-bearing zones to the pay zone.
- *Moving oil-water contact* – a uniform oil-water contact moving up into a perforated zone in a well during normal water-driven production can lead to unwanted water production.

- *Watered-out layer without cross-flow* – A common problem with multilayer production occurs when a high-permeability zone with a flow barrier (such as a shale bed) above and below is watered out.
- *Fractures or faults between injector and producer* – In naturally fractured formations under water-flood, injection water can rapidly break through into producing wells.
- *Fractures or faults from a water layer* – Water can be produced from fractures that intersect a deeper water zone.
- *Coning or cusping* – Coning occurs in a vertical well when there is an OWC near perforations in a formation with a relatively high vertical permeability.
- *Poor areal sweep* – Edge water from an aquifer or injection during water flooding through a pay zone often leads to poor areal sweep.
- *Gravity-segregated layer* – In thick reservoir layer with good vertical permeability, gravity segregation can result in unwanted water entry into a producing well.
- *Watered-out layer with cross-flow* – Water cross-flow can occur in high-permeability layers that are not isolated by impermeable barriers.

2.2 Impact of excessive water production

Excessive water production has a serious impact on field operations and the environment into which it is discharged. The produced water is either separated down-hole and injected into another formation, or brought together with oil to surface and separated there. Operational expenses, including lifting, separation, pumping, and reinjection add to overall cost of oil production. Once the water is separated from oil, it can be either re-injected into formation or disposed to the environment. The produced water after separation still contains minor parts of hydrocarbons, sand, metals and chemicals, which can plug the formation pores or create corrosion when re-injected, or can be harmful to the environment. Thus, in any case, the necessary treatment is a mandatory step to assure the safety side for operation and also conform to regulations. In 2002, produced water was estimated to cost the petroleum industry about USD 45 billion, annually (U.S. Department of Energy 2004). These costs include the expense to life, dispose of or re-inject produced waters, as well as the capital investment in surface-facility construction, and other environmental concerns (Bjørn, et al., 2011).

In addition, as the well ages, more water comes into borehole, building up the wells' hydrostatic pressure. In order to gain the same production as before, the pressure difference between bottom hole and wellhead need to be adjusted accordingly, either by increasing bottom-hole pressure or reducing wellhead pressure. At some point, when these two pressures reach their limits and can no longer be adjusted, the production rate will sharply decrease or the well will even "die". Gas-lift or down-hole pump can help to cure the well but extra cost will be added to operation.

2.3 Water control solutions

After the source/mechanism of excess water production is identified, the proper solution should be taken. The solutions to control water production correspond to each circumstance and can be defined as follow:

- Solutions to prevent early excess water production.
- Solutions to reduce the excess water production.
- Solutions for isolation pathway/ water shut-off.

2.3.1 Solutions to prevent early excess water production

The best solution for any problem is to prevent it before it happens. The solutions/techniques should be considered from planning/designing stage. Some of them are:

- Well-placement technology: enabling operators to optimize production or injection programs, improve reservoir performance, achieve higher extraction ratios, and reduce field-development and minimize water production (Schlumberger, 2001).
- Horizontal well: With this type of well, the problem with gas and water coning can be delayed due to larger drainage area in compare with vertical well (Wu, et al., 1995).
- Implementation of smart/intelligent wells: They allow for the completion of multiple reservoir intervals (zones) in a single wellbore. Each zone can be monitored and controlled individually from surface. If excess water entry from an oil-producing interval is indicated, an operator can shut in that interval while still producing from other zones without the need of running intervention equipment (Schiozer, et al., 2009).

- Design of perforation intervals: Design of type and perforation intervals in cased hole can also help to delay the gas and water coning.

2.3.2 Solutions to reduce excess water production

When the water breakthrough has already occurred, the excess water production keeps increasing with time. There are various solutions/techniques that can be applied to reduce the excess water volume brought to surface. By doing so, the operators can significantly reduce the total cost of lifting, surface facilities for produced water treatment, storage and re-injecting, thus the cost of the production of oil is greatly reduced. Reducing of excess water production also helps to reduce the environmental impact of oil and gas operation and environmental risk associated with re-injection wells. Some of popular techniques are:

- Downhole oil-water separation (DOWS): This technology is installed at the bottom of the well and separates oil and gas from water, and re-injects most of the water into another formation, which is usually deeper than the producing formation. DOWS effectively removes solids from disposal fluid and thus avoids solids plugging in the injected formation. These installations are often used in wells of little value, with a low oil production and a high water cut (Bowers, et al., 1998).
- Polymer injection: Water soluble polymer is injected to formation in order to increase viscosity and thus reduce mobility of injected water. Reduction of the water mobility helps to avoid early water breakthrough and improve sweep efficiency. This method is more effective in high heterogeneous formation and with high viscosity oil.

2.3.3 Solutions for isolation pathway/ water shut-off (WSO)

These solutions involve both mechanical and chemical methods/techniques, that can “shut off” water-bearing channels or fractures within the formation and prevent water from making its way to the well.

Mechanical Blocking Devices

Packers, plugs setting and cement are traditional techniques to solve ***near-wellbore*** problems, such as casing leaks, flow behind casing, rising bottom water and watered-out layers without cross-flow (Bedaiwi, et al., 2009).

In recent years, various new technologies with advantageous features have been presented giving very effective results for water shut-off. One of example is the PosiSet mechanical plugback tool, which can be deployed on coiled tubing or wireline and applied in both cased- and open-hole wells. PatchFlex technology with the advantages over traditional bridge plug (the inflatable sleeves are custom-built to match the length of the perforated intervals and can withstand wellbore cross-flow pressures. After setting, the sleeve becomes a composite liner inside the casing and can be re-perforated later to allow reentry to the zones) allows operator to shut off the water-producing zones and produce the new oil zones below them (Bailey, et al., 2000).

Water shut-off chemicals

If the mechanical blocking devices are mainly for near-wellbore problems, chemical solutions have a larger range of application in term of formation depth away from the wellbore and can address several water-type problems presented in section 2.3.1. By selection of chemicals system, chemicals can be either injected to near-well area to block the most water productive layers (with higher efficiency compared with mechanical techniques), or used as in-depth treatment to block high water permeability fractures/zones. They are injected as solutions and gels are formed within the reservoir. These gels are designed to be strong enough for long periods of time, at given formation temperature, salinity, and pH; they are also able to withstand the applied drawdown pressure during hydrocarbon production. This application is called profile modification or conformance control, which diverts injected water to un-swept zones and improves the distribution of injected fluids in heterogeneous reservoirs (Vafaie Sefti, et al., 2007).

With significant advantages such as flexibility for pumping without a work-over rig, high control of setting time, deeper penetrations into formation, ease of cleaving, lack of milling time, and an easy removal from the well-bore by water recirculation (Perez, et al., 1997), chemical solutions have become more used and more successful nowadays.

The chemicals most used for water shut-off are polymers and sodium silicate gels.

Polymeric gels are obtained by cross-linking high and/or low molecular weight polymers with crosslinkers (normally metal ion or metallic complexes). The chemical gelling solution (gelant) is prepared by adding the polymer to water, following by a crosslinker. Under a specific temperature and time, a crosslinking (gelation) reaction starts between the two components to form a three-dimensional cross-linked polymer network, which is referred as "gel". The two most commonly used polymers are partially hydrolyzed polyacrylamides (HPAM) and biopolymers (e.g., xanthan) (Karmakar, et al., 2006).

Silicate gels are created based on principle of reducing its pH. This is done by adding acidic activators to aqueous solution of sodium silicate. The use of silicate gels for petroleum application has arisen already in 1922, however its benefits and field potential were not really appreciated for a long time (Lakatos, et al., 2012). Vinot *et al.* (1989) listed several possible reasons why the operators do not appreciate the silicates. One of the reasons it was pointed out was that the mechanism of silicate gelation, particularly under reservoir conditions, is poorly understood. It's a premise for an increasing number of studies on silicates gel these days.

The main advantages of silicate gels are (Lakatos, et al., 1999):

- Low viscosity of treating solutions, viz. good placement selectivity.
- Short to moderate pumping time before onset of gelation.
- Flexible chemical mechanism.
- Good chemical and chemical stability.
- Excellent thermal and mechanical resistivity.
- Easy gel breaking in case of technical failures.
- Simple and cost-effective surface technology.
- Environmentally categorized as a "green" chemical

Various silicate-based technologies have been used several times worldwide. Field applications demonstrate ample examples for outstanding and positive statistic and lessons to learn (Lakatos, et al., 2012).

Algyő field (Hungary) is one large scale example of a successful water shutoff treatment using a combined silicate/polymer gel. . Until now (2012), more than 80 jobs were performed. The

statistical evaluation of program proved that 60-65% of the treatment was technically successful; meanwhile 40% of the jobs were economic. One of the most successful program brought a cumulative surplus of oil production totaled more than 100,000 t from 1981 until 1998 (Lakatos, et al., 2012).

In June of 2011, a single well pilot injection of sodium silicate in the Snorre field, offshore Norway, was carried out successfully. Acid hydrochloric acid (HCl) was used as activator in this job. An in-depth permeability restriction of approximately 40m away from the wellbore and permeability reduction of more than 100 were achieved and confirmed by post fluid infectivity measurements and transient falloff tests (Skrettingland, et al., 2012).

However, as any other systems, the silicate systems have also disadvantages-. (Lakatos, et al., 1999): state the following disadvantages:

- Gel is rigid and prone to fracture.
- Gel shows syneresis and thus reduces blocking efficiency.
- Silicates are prone to form precipitates instead of gel.
- Gelation time is hard to control.

Recognizing the disadvantages of the systems, various studies and tests have been performed to overcome the mentioned shortcomings; different additives was proposed and tested. For example, addition of acid phosphate into alkaline silicate reduced influence of salinity of formation water on the gelling time (Beecroft, 1969); the gelation of a silicate system still happened even though the pH remained constant (>11) when adding hydrolysable esters into the alkaline silicate solution as a dispersed phase (micro-emulsion) (Vinot, et al., 1989); Glyoxal and urea were also tested as gelling agent (activator) for sodium silicate gelling system. These works have also shown that as a result of a unique gelation mechanism, the properties of gel and the chance to have permanent and efficient barrier formation under harsh reservoir conditions were significantly improved (Lakatos, et al., 1999).

3 Theoretical Background

In this section the required theoretical background for this study is discussed. A short description about chemistry of sodium silicate, then how the silicate gel is formed using which gelling agents are presented sequentially. Then influential factors to silicate gel kinetics are identified in order to derive a general equation for sol-gel transition time. Evaluation of gel strength and gel syneresis is also explained. A section of basic rheological concepts is presented at last.

3.1 Chemistry of sodium silicate

Sodium silicate is manufactured by heating silica and sodium carbonate to temperatures above 1300°C to form a water-soluble glass referred as “water glass” (Iler, 1979).

The sodium silicate chemistry is complex and not fully understood, but according to Iler (1979) the following fundamental equilibria are involved:

$$SiO_2 + H_2O = Si(OH)_4 \tag{3.1}$$

$$Si(OH)_4 + OH^- = HSiO_3^- + H_2O \tag{3.2}$$

$$2HSiO_3^- = Si_2O_5^{2-} + H_2O \tag{3.3}$$

$$Si_2O_5^{2-} + H_2O = HSi_2O_6^{3-} + H^+ \tag{3.4}$$

$$HSiO_3^- + OH^- = SiO_3^{2-} + H_2O \tag{3.5}$$

Generally, sodium silicates are identified by the SiO_2:Na_2O ratio, *n*. Alkalinity increases by decreasing *n*. The commercial sodium silicates are produced as glasses having *n* varying in the range of 1.6 to 3.9.

At a given ratio, the density of a solution is dependent on total solids content. The higher the ratio is, the lower the density at a given concentration. The viscosity of a sodium silicate solution is a function of concentration, density, ratio and temperature. The viscosity strongly increases when ratio increases.

3.2 Gel formation

The pH of commercial silicate solutions ranges from approximately 10 to 13, depending on the $SiO_2:Na_2O$ molar ratio. The stability of a sodium silicate solution depends to a large extent on pH. All sodium silicate solutions will polymerize to form a silica gel when the pH value is reduced below 11. The development of the gel can be described with the following steps (Iler, 1979):

1. Polymerization of monomer to form particles.
2. Growth of particles.
3. Linking of particles together into branched chains, then networks, finally extending throughout the liquid medium, thickening it to a gel.

Succeeding steps in polymerization from monomer to large particles and gel or powder have been represented schematically by Iler (1979) as in Figure 3.1.

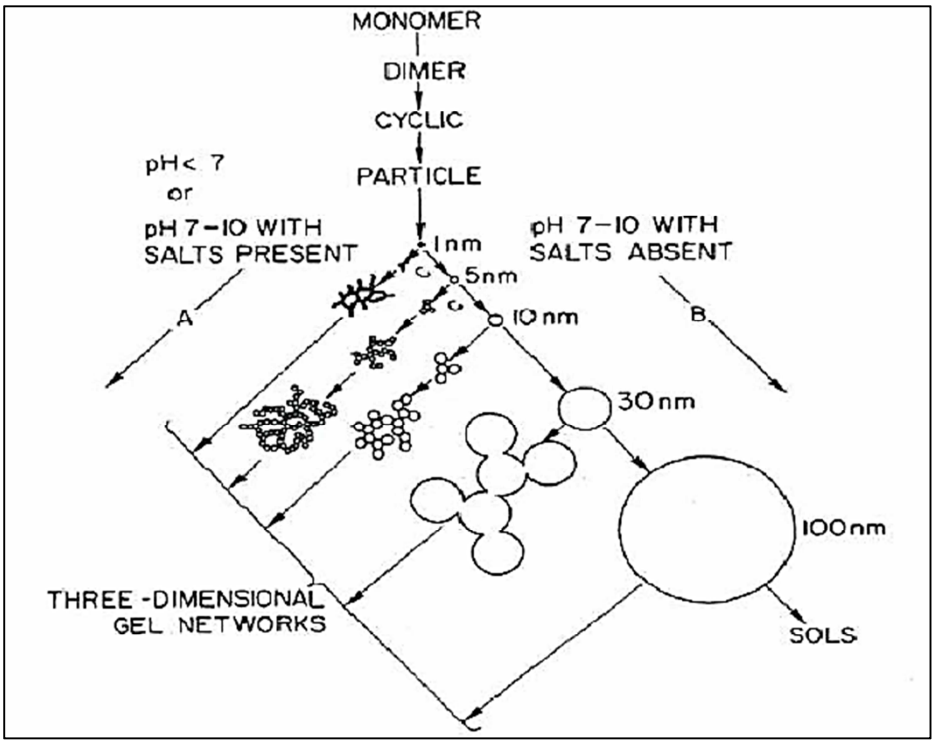

Figure 3.1. Schematically illustration of polymerization of silica (Iler, 1979)**.**

In basic solution (B) particles in sol grow in size with decrease in numbers; in acid solution or in presence of flocculating salts (A), particles aggregate into three-dimensional networks and form gels (Iler, 1979).

Water molecules are captured and locked in a network of silicate molecules. There are many configurations of polymerization. One simplified configuration is presented in Figure 3.2 (Bol, et al., 1998). The degree of the polymerization increases as the processes move down.

The rate and extent of sodium silicate polymerization is affected by several factors. To understand and control gelation time, we should take these factors into the account and know in which direction they affect the gel system. These factors are presented below:

- pH: When the pH of solutions decreases, the polymerization process happens faster.
- Molar Ratio: An increase in silica ratio results in higher degree of polymerization.
- Dilution rate: At a constant pH, dilution de-polymerizes silica, the polymerization process occurs more slowly.
- Salts: Act as catalysts and increase the rate of polymerization.
- Temperature: Gelation process is accelerated at higher temperatures.

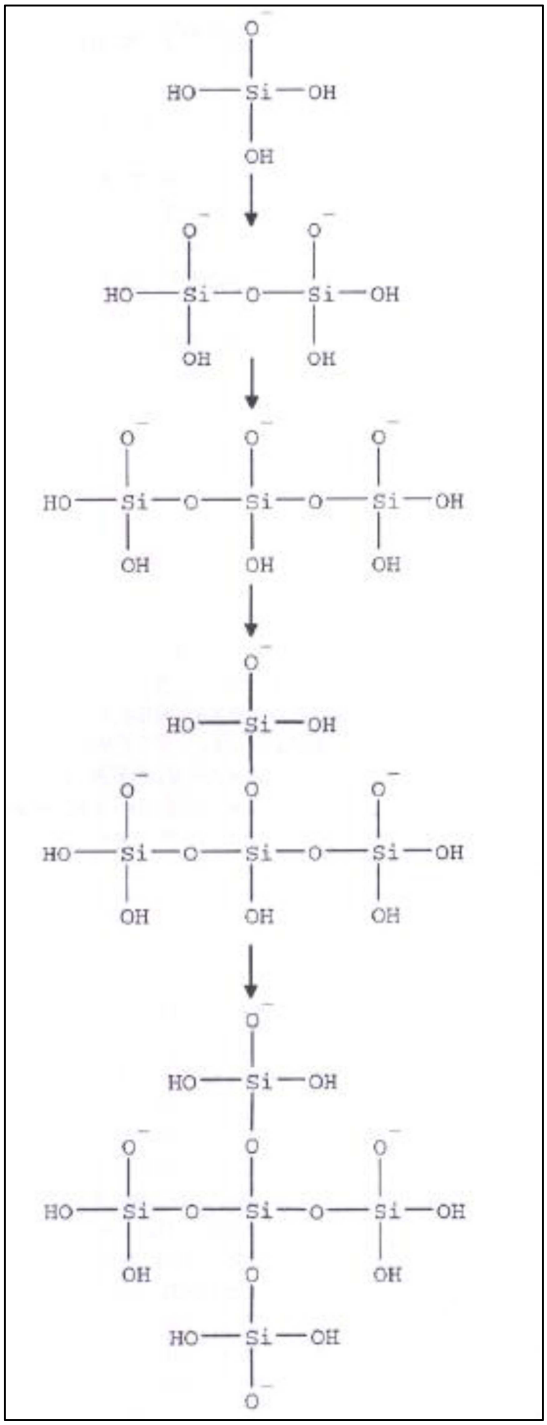

Figure 3.2. Simplified silicate polymerization (Bol, et al., 1998).

3.3 Gelling agents

Decreasing the pH will initiate the gelling process of sodium silicate solution. The simplest way to reduce pH of the solution is to add the acid. Such systems have been applied for many years and a lot of work has been done on optimizing silicate/acid systems water control purposes (Stavland, et al., 2011).

Despite the fact that acids have been widely used, there are plenty of other chemicals that can be used as gelling agents. Krumrine *et al.* (1985) presented an overview of such agents (see Table 3.1).

In this work, a silicate/alkali metal salt system was studied. Since the gelling agent is a type of salt, this system is considered to be safer than acidic gel system. The salt solution is easy to prepare and was used in this work at concentration 1M.

Table 3.1. Gelling agents for sodium silicate (Krumrine, et al., 1985)**.**

Type	Compound(s)	Examples
Inorganic	Acids	HCl, H_2SO_4, HNO_3
	Ammonium Salts	$(NH_4)_2CO_3, (NH_4)_2SO_4, NH_4Cl$
	Alkali Metal Salts	$Na_2ZnO_2, NaHSO_4, KF, K_2ZnO_2, NaCl$
	Polyvalent Metal Salts	Cations Al, B, Ti, Zr, Fe, Cu, Si with anion $HCO_2^-, CH_3CO_2^-, OH^-$
Organic	Acids	Formic, acetic, propionic and corresponding Al, Ba, Ca, Mg, Zn salts
	Aldehydes	Formaldehyde, paraformaldehyde, glyoxal, benzaldehyde
	Polyhydric Alcohols	Ethyleneglycol, dextrin, cellulose, glycerin, starches, sugars
	Esters, Amides, Lactones	Ethylacetate, ethyl chloroformate, formide dimethylformide
	Polymers	Polystyrene, dipolvynilbenzene, polyester resins, latex polyvinyl alcohol
	Surfactants	Most nonionic and many anionic surfactants
Natural Minerals	Organic Compounds	Proteins, polypeptides, gelatins, asphalt
	Inorganic Compounds	Clay, fly ash, shale, gypsum, sulfur

3.4 Silicate gel kinetics

One of the main objectives of this work is to define a unified sol-gel transition time correlation that describes the relationship between sol-gel transition time and formation parameters (e.g., temperature, water salinity, presence of divalent ions, amount of sodium silicate and activator) that affect the gel system. That equation can then be used to design the silicate gel system for field applications under specific reservoir conditions and operator objectives.

As mentioned earlier, sol-gel transition time is a function of several variables. A unified sol-gel transition time correlation which describes the sol-gel transition time for silicate gel system will be derived in this work with respect to the following variables:

- Sodium silicate solution concentration;
- Activator concentration;
- Temperature;
- Divalent ion concentration: Ca^{2+} and Mg^{2+}.

Stavland *et al.* (2011) derived a general equation of bulk gelation time for silicate gel system, which was formed by a sodium silicate solution with hydrochloric acid HCl 2M as activator. The equation has the following form:

$$t_g = A \times e^{\alpha[Si]} \times e^{\beta[HCl]} \times e^{\gamma\sqrt{[Ca^{2+}]}} \times e^{E_a/RT} \quad (3.6),$$

where t_g – gelation time (days);

A – multiplication factor, $A = 2.1 \times 10^{-8}$;

[Si] – silicate concentration (wt%);

[HCl] – concentration of hydrochloric acid 2M (wt%);

[Ca^{2+}] – concentration of calcium ion (ppm);

E_a – activation energy (kJ/mol), $E_a = 77\ kJ/mol$;

R – gas constant (kJ/mol·K), $R = 8.314\ kJ/mol \cdot K$;

T – absolute temperature (K);

$\alpha,\ \beta,\ \gamma$ – empirical constants, $\alpha = -0.6, \beta = -0.7, \gamma = -0.1$.

Noted that the "gelation time" referred by the authors in Equation (3.6) is defined as the time at which the gelant solution was characterized as gel 3 in a gel code system (see Table 4.2). This gel code classification will be described in more details in section 4.2.

Equation (3.6) was formed by combining all functions which describe the effects of each individual factor on gelation time. The exponential equation was used by Stavland *et al*. (2011) in all cases since it was provided the best agreement with the experiment results.

Based on the concept of Equation (3.6), a unified sol-gel transition time correlation will be developed for the silicate gel system considered in this work, which will include all functions that describe the effects of each individual factor on sol-gel transition time as follows:

$$t_{sg} = A \times f([SS]) \times f([Ac]) \times f([Ca^{2+}]) \times f([Mg^{2+}]) \times e^{E_a/RT} \quad (3.7),$$

where t_{sg} – sol-gel transition time (hrs);

A – matching coefficient;

[SS] – concentration of sodium silicate solution (wt%);

[Ac] – concentration of activator (wt%);

[Ca^{2+}] – concentration of calcium ion (ppm);

[Mg^{2+}] – concentration of magnesium ion (ppm).

Equation (3.7) is formed from five individual functions, where the sol-gel transition time is a function of only one factor, while the others are kept constant.

1. Sol-gel transition time as a function of sodium silicate solution concentration:

$$t_{sg} = f([SS]) \quad (3.8)$$

2. Sol-gel transition time as a function of activator concentration:

$$t_{sg} = f([Ac]) \quad (3.9)$$

3. Sol-gel transition time as a function of ion Ca^{2+} concentration:

$$t_{sg} = f([Ca^{2+}]) \quad (3.10)$$

4. Sol-gel transition time as a function of ion Mg^{2+} concentration:

$$t_{sg} = f([Mg^{2+}]) \quad (3.11)$$

5. Sol-gel transition time as a function of temperature:

$$t_{sg} = \xi \cdot e^{E_a/RT} \quad (3.12),$$

where ξ - empirical constant.

For most chemical reactions, it is common to assume that the temperature dependency is given by the Arrhenius equation (Stavland, et al., 2011).

All five functions are determined experimentally based on experiment results. However the matching coefficient A is obtained by matching the measured data to the unified sol-gel transition time correlation.

In order to find these functions, the sol-gel transition time has to be measured for different sodium silicate solution and activator concentrations. Additionally, calcium and magnesium content in the makeup water has to be varied. Some of these experiments have to be done for different temperatures to estimate the effect of temperature on time of gelation initiation.

3.5 Gel strength

After prepared at surface, the silicate gel solution will be injected into formation. The required injected volume and injection time are calculated based on sol-gel transition time, desired effective distance, available pumping rate, and well injectivity. After injection, the well will be shut-in for certain period of time, in the depending of the sol-gel transition time and the desired gel strength. The formed gel must be strong enough to withstand the injection pressure when the flow is resumed.

This work is aimed to assist in the design a water shutoff treatment at an injection well in a *naturally fractured formation*. A ***minimum pressure gradient*** must be applied to initiate the gel extrusion through the fracture or in other words, to make gel "flow". This pressure gradient suggests the gel material exhibits a yield stress. In the low deformation range, the material exhibits a stable, solid-like structure which displays elastic behavior. But when the deformation exceeds the tolerance, the structure is destroyed and the material flows (Wang, et al., 2006). For a gel with yield stress, τ_y, under stationary (steady state) condition, Bird *et al*. (1983) used a simple force balance to calculate the minimum pressure gradient, dP/dl, required for gel to extrude through two smooth parallel plates separated by distance w (see Appendix B):

$$dP/dl = 2\tau_y/w \tag{3.13}$$

From this minimum pressure gradient, the ***maximum differential pressure the formed gel can withstand*** is:

$$dP_{max} = \frac{2\tau_y}{w} dl \tag{3.14}$$

The yield stress of formed gels will obtained from laboratory experiments.

3.6 Gel syneresis

Syneresis is a process, in which the formed silicate gel after a certain period of time tends to contract, expelling water. This process clearly will affect the long-term effectiveness of a silicate treatment. This phenomenon is most pronounced at high silicate concentrations and/or high temperatures (Vinot, et al., 1989).

The target for this silicate gel application is a mature oil field, which has been producing for a long time under water flooding. The target production well produces at high water cut levels and the only residual oil exists in the region of silicate gel deployment. Under this condition, the gel syneresis is expected to be very low, almost insignificant, thus this effect was not considered in this work.

3.7 Basic Rheological concepts

Rheological experiments do not merely reveal information about flow behavior of liquids but also about deformation behavior of solids. The connection here is that a large deformation produced by shear forces causes many materials to flow (Mezger, 2011).

Silicate gels display a viscoelastic behavior, meaning that their properties are intermediate between those of elastic solids and viscous liquids. Oscillatory test are chosen in this work since it is used examine all kinds of viscoelastic materials, from low-viscosity liquids to polymer solutions and melts, dispersions, gels, and even rigid solids.

For an elastic solid, application of a shear stress, τ, causes the solid to deform by a “strain” or distance, γ. If the stress it not too large, the solid relaxes to its original shape after the stress is

removed. When performing oscillatory tests on ideally elastic materials, i.e completely inflexible, stiff ad rigid solids, Hooke's law applies as follows (Mezger, 2011):

$$\tau(t) = G^* \cdot \gamma(t) \tag{3.15},$$

with the **complex shear modulus G*** and the time dependent values of the sine functions of τ and γ. G* can be imagined as the rigidity of the test materials, i.e. as the resistance against deformation.

Since $G^* = \tau(t)/\gamma(t) =$ const, the $\tau(t)$-curve is always "in phase" with the $\gamma(t)$-curve, i.e both curves are occurring without any delay between preset and response in the form of sine curves.

The time derivative of the sinusoidal strain function $\gamma(t)$ results in the strain rate (or shear rate) function $\dot{\gamma}(t)$ which occurs in the form of a cosine function.

If a solid is deformed significantly, the deformation may become plastic, meaning that the solid will not completely relax to its original shape after the stress is released (Callister, 1997). For common solids, the point (stress) at which plastic behavior begins is labeled as the **yield point** (or **yield stress**).

For a viscous fluid, no elastic deformation occurs when a shear stress is applied. Instead, the fluid flows dispersing the applied force and energy as heat (Macosko, 1994). When performing oscillatory tests on ideally viscous fluids, Newton's law applied as follows (Mezger, 2011):

$$\tau(t) = \eta^* \cdot \dot{\gamma}(t) \tag{3.16},$$

with the **complex viscosity $\boldsymbol{\eta}^*$**, and the time-dependent value of the sine functions of τ and $\dot{\gamma}$. η^* can be imagined as th viscoelastic flow resistance of a sample.

Since $\eta^* = \tau(t)/\dot{\gamma}(t)$ = const, the $\tau(t)$-curve is always "in phase" with the $\dot{\gamma}(t)$-curve, i.e. both curves are appearing without any delay between preset and response, showing the same frequency.

For a viscoelastic material, elements of both elastic and viscous character are exhibited (Macosko, 1994).

A common method to assess the viscoelastic nature of materials uses measurement of stresses during the application of a sinusoidal oscillating shear strain. Formally, the sinusoidal strain (or deformation) function is presented by (Mezger, 2011):

$$\gamma(t) = \gamma_o \cdot sin\omega t \quad (3.17),$$

with the shear strain amplitude γ_o(%), and the angular frequency ω in (rad/s) or in (s^{-1}).

With the presetting shear strain γ as in equation (3.17), the measuring result τ-curve will have the following form (Mezger, 2011):

$$\tau(t) = \tau_o \cdot sin(\omega t + \delta) \quad (3.18),$$

with the phase shift angle δ between the preset and the resulting curve, which is usually specified in degrees (^{o}) or rarely in rad.

For ideally elastic behavior $\delta = 0^o$, for ideally viscous behavior $\delta = 90^o$ and for viscoelastic behavior, the stress wave will be shifted by an intermediate phase angle $0^o < \delta < 90^o$ (Mezger, 2011).

The curves in Figure 3.3 illustrate strain wave $\gamma(t)$, strain rate wave $\dot{\gamma}(t)$ and shear stress wave $\tau(t)$.

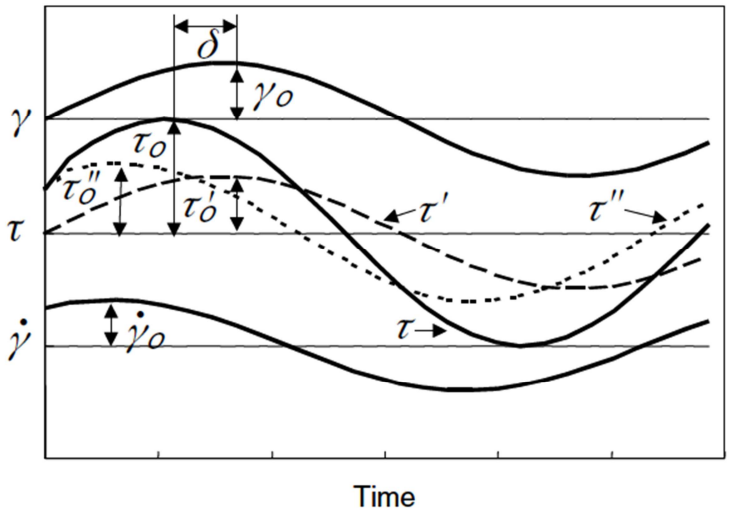

Figure 3.3. Illustration of dynamic measurements **(**Macosko, 1994**).**

The stress wave, $\tau(t)$, is generally separated into two waves with the same frequency. One wave, $\tau'(t)$, is in phase with the strain wave, while the other wave, $\tau''(t)$, is 90^o out of phase with the strain wave. In this way, the stress wave is separated into an elastic component and a viscous component (Macosko, 1994).

Elastic or storage modulus G' is a measure of the deformation energy stored by the sample during the shear process. G' represents the ***elastic behavior*** of a material and is defined by (Mezger, 2011):

$$G' = \tau_o'/\gamma_o \tag{3.19}$$

Loss modulus G" is a measure of the deformation energy used up by the sample during the shear process and therefore afterwards, it is lost for the sample. G" represents the ***viscous behavior*** of a test material and is defined by (Mezger, 2011):

$$G'' = \tau_o''/\gamma_o \tag{3.20}$$

The phase angle or loss angle, δ, is related to *G'* and *G"* through Equation 3.21:

$$tan\delta = G"/G' \qquad (0^o \leq \delta \leq 90^o) \tag{3.21}$$

As indicated in Figure 3.3, the τ' wave is in phase with the strain (γ) wave, while the τ'' wave is in phase with shear rate ($\dot{\gamma}$).

The complex viscosity, $|\eta^*|$, is defined by (Mezger, 2011):

$$|\eta^*| = \sqrt{(\eta')^2 + (\eta'')^2} = \sqrt{(G''/\omega)^2 + (G'/\omega)^2} \tag{3.22}$$

Complex viscosity can be interpreted as the apparent viscosity of viscoelastic solution/materials, which are composed of both an elastic and viscous portion.

The complex modulus, $|G^*|$, is defined by (Mezger, 2011):

$$|G^*| = \sqrt{(G')^2 + (G'')^2} = \tau_o/\gamma_o = |\eta^*|\omega \tag{3.23}$$

In this work, rheology measurements of silicate gel system were performed in order to obtain the rheology properties, thus define gelation time of gel system and gel strength according to time.

4 Laboratory Equipment and Experimental Procedures

In this section, the equipment and chemicals that were used in this work will be presented and measurement modes used are also explained in brief.

4.1 Chemicals and equipment

In all experiments, a commercial sodium silicate solution system was used which contains 15 wt% of sodium silicate. The activator was prepared according to requirements of the achieved sol-gel transition time. The density of sodium silicate solution and activator was measured and their values were 1.097 g/cm^3 and 1.038 g/cm^3, respectively. In all the experiments, except ones in section 5.2, the concentrations of chemicals in samples are represented in weight percentage.

A thin layer of approximate one milliliter (1 ml) thickness of n-decane was added on the top of the sample to minimize evaporation. It is expected that the presence of n-decane with the gelant system in the described form will have no impact on the gelation process, sol-gel transition time, and properties of the created gel. This hypothesis was tested with experiments which were performed on two samples and described later in Section 5.1.

The Anton Paar Rheometer MCR 302 was used in this study to measure the rheological properties of all samples prepared. The concentric cylinder measuring system CC27, also called bob/cup system was used in all measurements. CC27 consists of an inner cylinder (bob) and an outer cylinder (cup). During the experiments, the bob is set in motion by the setting parameters from the user while the cup remains stationary. The motion of the bob is dictated by the input parameters selected from the user. This measuring system requires a sample volume of 19 ml.

The temperature control is ensured by a Peltier system, providing rapid heating and cooling with accuracy of 0.01^{o}C. A solvent trap ST-CYL-C/Q1 was used to minimize evaporation of the sample, especially at high temperatures. Solvent trap includes an upper and a lower part, which should be placed at a reasonable distance to avoid contact that will create friction between them; they should also be not too far away from each other since the solvent trap will lose its functionality.

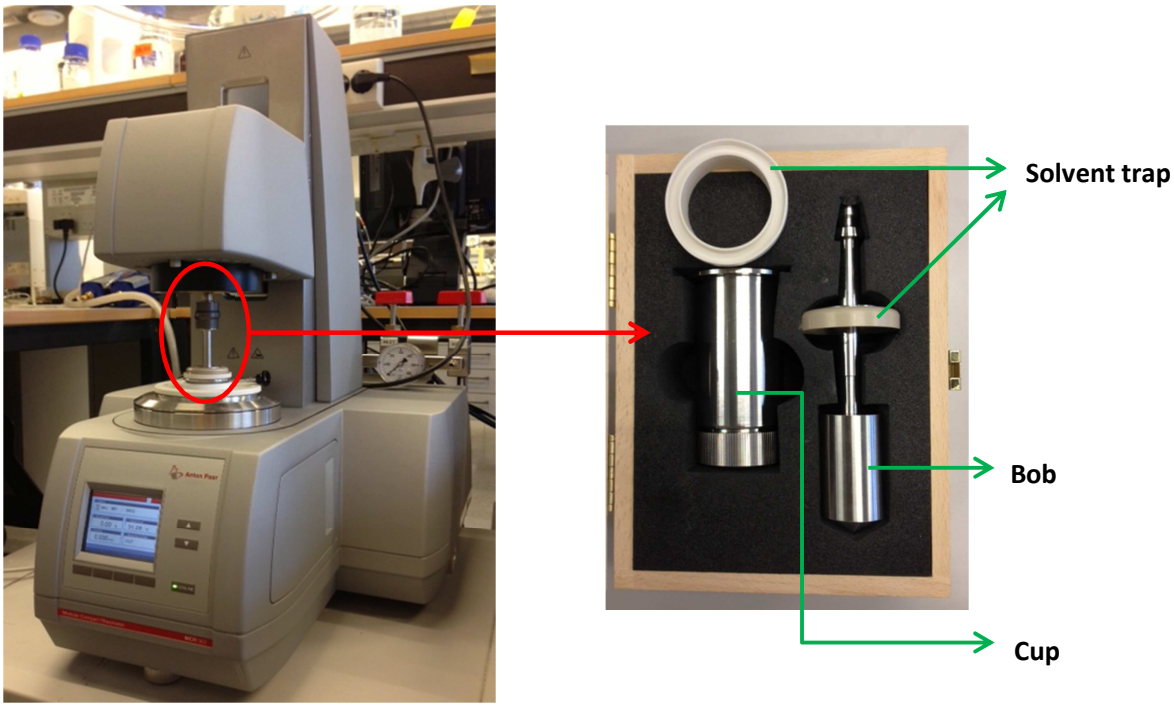

Figure 4.1. Anton Paar Rheometer MCR302: the measuring system CC27 along with the solvent trap.

4.2 Measuring modes

All samples were undergone through two oscillation test modes in the order presented below:

1. **Dynamic-Mechanical Analysis (DMA) Test Mode** – This test was run in in order to determine the **"gel point"**. Temperature is kept constant during a given DMA test, i.e., all tests conducted at isothermal conditions. During this test, the sample is subjected to a controlled shear strain $\gamma(t) = \gamma_o \cdot sin\omega t$, with:
    - a constant angular frequency $\omega = 10\, rad/s$, and
    - a constant oscillatory strain $\gamma_o = 1\%$.

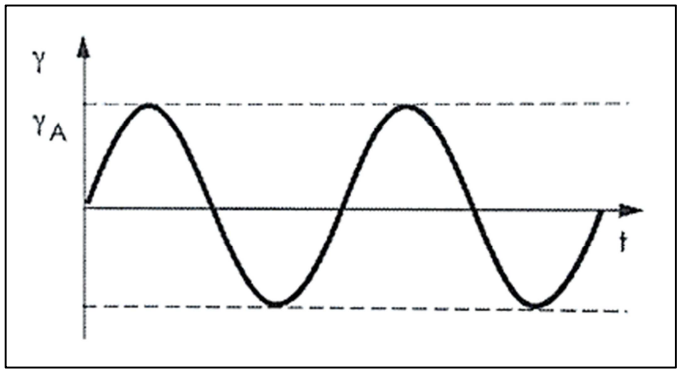

Figure 4.2. Preset of an oscillatory test with a constant amplitude and a constant frequency, here with controlled strain (Mezger, 2011)**.**

These two parameters show how fast and how much, respectively, the bob turns during the test. They were chosen based on the recommendation given by Mezger (2011).

The oscillatory strain recommendation of $\gamma_A \leq 1\%$ was tested to verify if the chosen strain value is appropriate for the gel system under consideration.

DMA tests on three samples with 24 g of sodium silicate solution and 6 g of activator at different oscillatory strains of 0.1%, 1% and 10% were performed to confirm the chosen strain value. The measured viscosity curves of the three samples are presented in Figure 4.3. Note that the y axis represents the complex viscosity of tested samples.

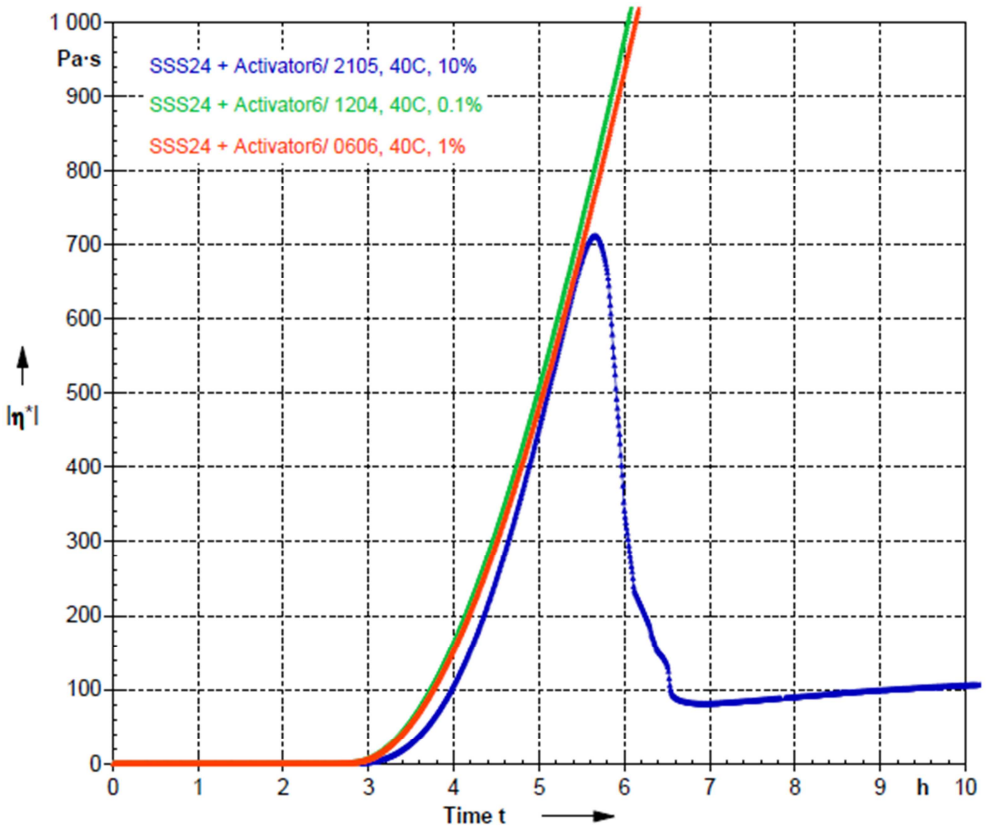

Figure 4.3. Viscosity vs. time of three samples measured during a DMA test conducted at three strain amplitudes.

The sharp increase of the measured viscosity indicates the start of gelation time or transition from sol to gel. Figure 4.3 shows that the starts of gelation at strain amplitudes of 0.1% and 1% were very close to each other, which mean that the gel system behaves practically the same way under these applied strains. The sample that was exposed to a 10% strain took a bit longer time to start gelling probably due to the fact that it was exposed to a larger deformation, which yielded larger disturbances to the sample. In addition, due to this large deformation, the formed gel broke around 5.6 hours, peak on viscosity curve, with a subsequent sharp reduction of the measured viscosity (note that the gel tends to slightly recover its viscosity after 6.6 hours but it never returns the viscosities prior to its break). Obviously, the applied strain value of 10% should not be used for the silicate solution under investigation. Concluding, these tests confirm the choice of a strain value (1%) for the DMA test conducted in this work.

Another requirement for the oscillatory strain is that it must be within the LVE (Linear Visco-Elastic) range. The selected value of 1% satisfied this condition as confirmed by the results from the second mode test. Finally, as shown in Appendix A, the oscillatory strain can be converted into deflection angle using the formula:

$$\varphi = 81.1 \cdot 10^{-3} \cdot \gamma = 81.1 \cdot 10^{-3} \cdot 0.01 = 0.811 \cdot 10^{-3}\ rad = 0.811\ mrad \sim 0.05^{o}.$$

This states that for the selected 1% oscillatory strain of 1%, the bob turns around only by 0.5^{o} during the DMA test, indicating a very small deformation applied to the sample.

There are several methods reported in literature to define the gelation time. Sydansk (1990) proposed the ***bottle testing method***, which provides a semi-quantitative measurement of gelation rate and gel strength. In this method, the developed gel strength was expressed with the use of an alphabetic code, of A through J, shown in Table 4.1. The normal procedure followed is as follows: (a) gelant solution is formulated and placed in the bottle at a specific temperature, (b) the bottle is inverted during each reading time at different intervals and the gel strength codes are recorded, and (c) gelation time is considered as the time when change is no longer observed in the gel strength code (Vafaie Sefti, et al., 2007).

Table 4.1. Bottle-test gel strength codes (Sydansk, 1990)**.**

A	No detectable gel formed.
B	Highly flowing gel.
C	Flowing gel.
D	Moderately flowing gel.
E	Barely flowing gel.
F	Highly deformable non-flowing gel
G	Moderately deformable non-flowing gel.
H	Slightly deformable non-flowing gel.
I	Rigid gel.
J	Ringing rigid gel.

The bottle testing method was used by Stavland *et al.* (2011) for establishing the gelation time of a silicate solution, but the authors proposed a simpler coding system, which contains only 4 gel codes, to describe the gel context and to determine the degree of gelation as shown in Table 4.2. Stavland *et al.* (2011) reported the gelation time as the time at which the gelant solution was characterized by one of the gel code in this table.

Table 4.2. Classification of gel codes (Stavland, et al., 2011).

Gel code	Description
0	Clear and low viscous fluid
1	Cloudy and low viscous fluid
2	Cloudy and high viscous
3	Rigid gel

Note that the accuracy of bottle testing method depends heavily on the gelation time definition (letter or code) used as well as on the testing frequency.

Al-Anzi *et al.* (2011) implemented the ***static shear method (viscometer)***, with the viscosity of each gelant solution recorded versus time by a viscometer and defining the gelation time at the time (point) on the graph where the solution viscosity started to build up sharply. Figure 4.4 shows one example from their work of the graphical determination of the gelation time. As Figure 4.4 demonstrates, sometimes it is very difficult to define the point of a sharp viscosity increase, especially for the solution represented by the black square points. The static shear method is more accurate compared to the bottle testing one, but it is not so easy in keeping consistency when defining the gelation point.

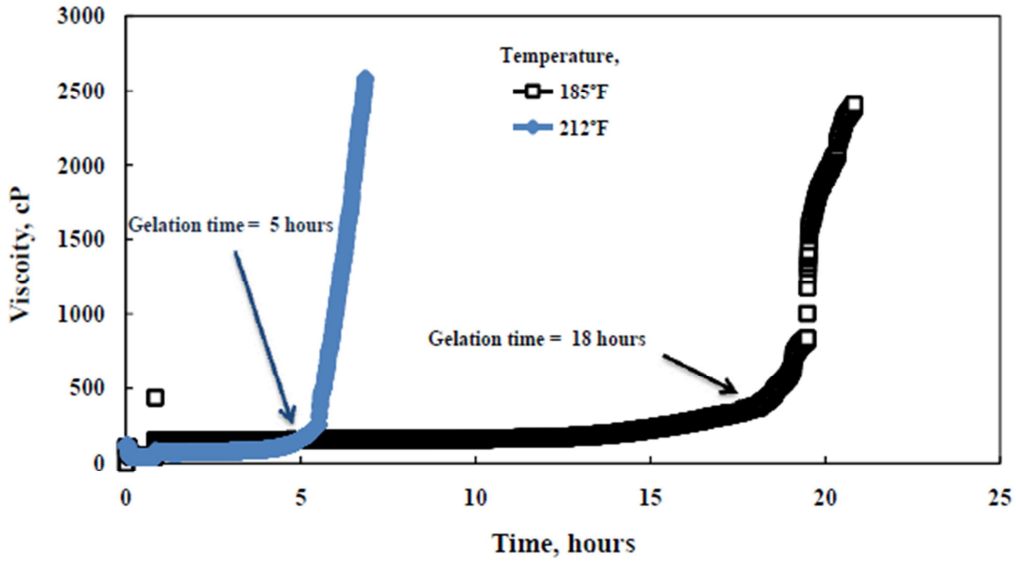

Figure 4.4. Viscosity of WSO (water shut-off) system as a function of both time and temperature at 40 s^{-1} (Al-Anzi, et al., 2011)***.***

The two described methods – bottle test and static shear using viscometer – clearly do not give the same gelation time when used in the same solution. The same word "gelation time" is used but it represents different stages of the gelation process in each method.

In this work, a more accurate and consistent method is proposed, the ***dynamic shear method***, in defining the sol-gel transition time (often referred by some authors, e.g., Al-Anzi *et al*. (2011) as the gelation time), using the Anton Paar Rheometer. However, in this work instead of "gelation time" (where the solution already achieves some degree of gelation), the transition time (t_{sg}) is recorded when the solution transitions from sol-to-gel at the onset of gelation process. The principal of this method is explained as follows: Initially before the gel forms, the sample displays the behavior of a liquid with G" > G', therefore the sample is still in the sol state. At the transition point, the gel starts to set with G' > G", and the sample display more-and-more a gel-like and eventually solid-like behavior. The time point t_{sg} at the intersection of the curves of G' and G" indicates the sol/gel transition point, or briefly, the "gel point". At this time G' = G" or tanδ = G"/G' = 1 (Mezger, 2011). The gel point can be detected accurately by using the measured G' and G'' values versus time.

The left panel of Figure 4.5 shows the recorded storage modulus G', loss modulus G'', and phase angle δ values versus time during a DMA test on a silicate solution system. The right

panel in Figure 4.5 presents the measured viscosity curve versus time. It should be noted that the gel point on the left panel corresponds to the point of sharp change of viscosity curve on the right panel.

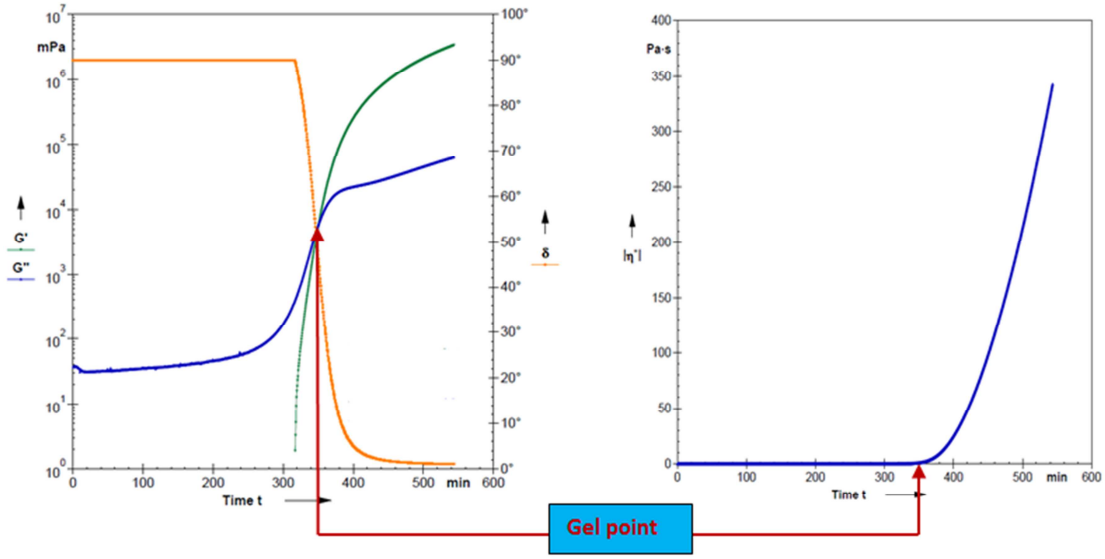

Figure 4.5. Determination of gel point.

2. **Amplitude Sweep (AS) Mode** – During this test, the sample is subjected to an increasing oscillatory strain (0.01% to 1000%) in a logarithmic ramp profile, while the angular frequency and temperature are kept constant ($\omega = 10\ rad\ s^{-1}$). The measured storage and loss moduli, G' and G", are examined as a function of strain. Amplitude sweeps are mostly carried out for the sole purpose of determining the limit of the LVE range, which defines the ***limiting shear strain*** $\boldsymbol{\gamma_L}$ of a formed gel.

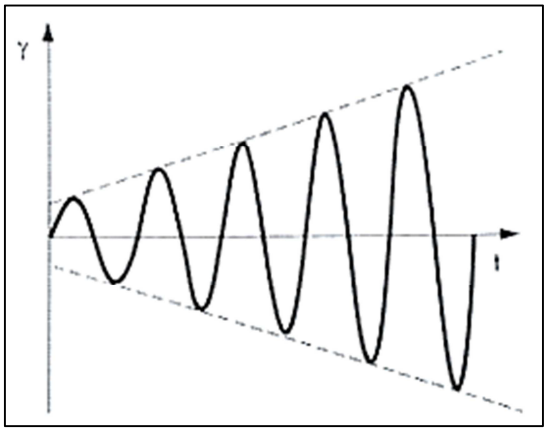

Figure 4.6. Preset of a shear strain amplitude sweep, or briefly, strain sweep (Mezger, 2011).

The limiting shear strain γ_L represents the largest deformation or shear strain amplitude, below which the measured storage and loss moduli G' and G" retain a constant plateau value, i.e., the sample structure is preserved. For $\gamma > \gamma_L$, the structure of sample has been already changed irreversibly, or it is even completely destroyed (Mezger, 2011). γ_L is defined either by onset of a decrease noted on curves G' and G" plotted versus shear strain (Figure 4.7) or by a significant increase in the G" curve (Figure 4.8) over a preset range of the tolerated deviation, e.g., as 5% or 3% (or even 10%). The used defines the desired range of tolerance, then the γ_L value is to be determined by the analysis program. In this work, since the G' and G" curves, plotted as a function of shear strain, of the examined gelant solutions showed a similar behavior to the one depicted on Figure 4.7 b with the G" curve always having the tendency to deviate from plateau value before the G' curve, the γ_L was defined as the strain amplitude at which G'' deviates by 5% from its plateau value.

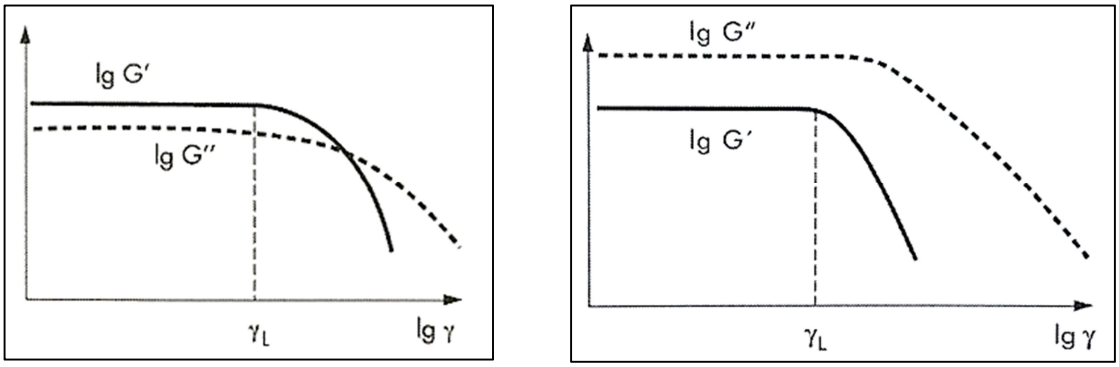

a) b)

Figure 4.7. Strain amplitude sweep of a) a sample showing gel-like character in the LVE range, i.e. G'>G"; b) a sample showing the character of a viscoelastic liquid in the LVE range, i.e. G">G' (Mezger***, *2011*).***

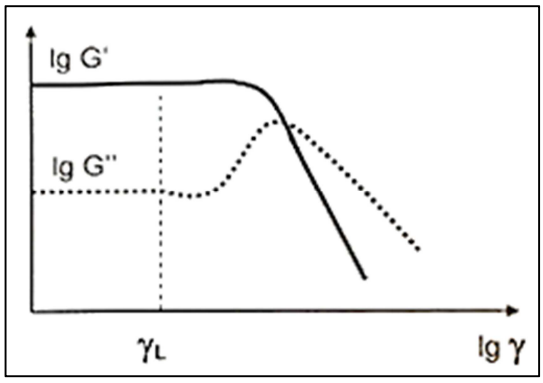

Figure 4.8. Strain amplitude sweep of a sample showing G" – peak (Mezger, 2011)***.***

The limiting shear strain γ_L is associated with a critical shear stress τ_y. This critical shear stress is also called "***yield stress***" or "***yield point***". No significant change of the internal structure occurs as long as stresses below the yield point are applied, and therefore, no yielding behavior or deformation can be observed in this range. In this work, τ_y was determined as the shear stress that corresponds to the estimated limiting shear strain, γ_L, as shown in Figure 5.4 in the next chapter. From the yield stress value one can estimate the pressure gradient required for the formed gel to be extruded through a formation fracture (see Section 5.10).

The AS mode was run on the same sample after the gelation has occurred and the gel reached a substantially higher viscosity than the original silicate system. The output values of this test depend on the post gel-point time the sample is tested, since its viscosity, and thus the structure of the gel, grows with time.

5 Results and discussions

This section describes the experiments that were carried out in this work; the results obtained, as well relevant discussions associated with the laboratory observations. The experiments are grouped according to the objective of each experiment series. All samples in each experiment group were tested under both test modes, which were described on section 4.2. Data analysis and discussion are presented at the end of each group of experiment.

5.1 Examine the effect of n-decane on sol-gel transition time

As discussed in section 4.1. Chemicals and equipment, a thin n-decane layer of approximately 1 ml thickness was added at the top of the sample to minimize evaporation. This section tests the hypothesis that the addition of n-decane will have no impact on the gelation process, sol-gel transition time, and properties of the created gel.

Two samples with the same composition namely, 22 g of sodium silicate solution and 8 g of activator were tested in DMA mode and at temperature of 20^{o}C to investigate any impact of n-decane on the sol-gel transition time. Solvent trap was used in both experiments but n-decane was added on top of only one of the samples. Two experiments were conducted at room temperature (20^{o}C) to make sure that the absence of n-decane, in one the experiments, will not cause significant water vaporization, which will create uncertainties on the estimated sol-gel transition time. The viscosity curves obtained from two experiments are plotted in Figure 5.1.

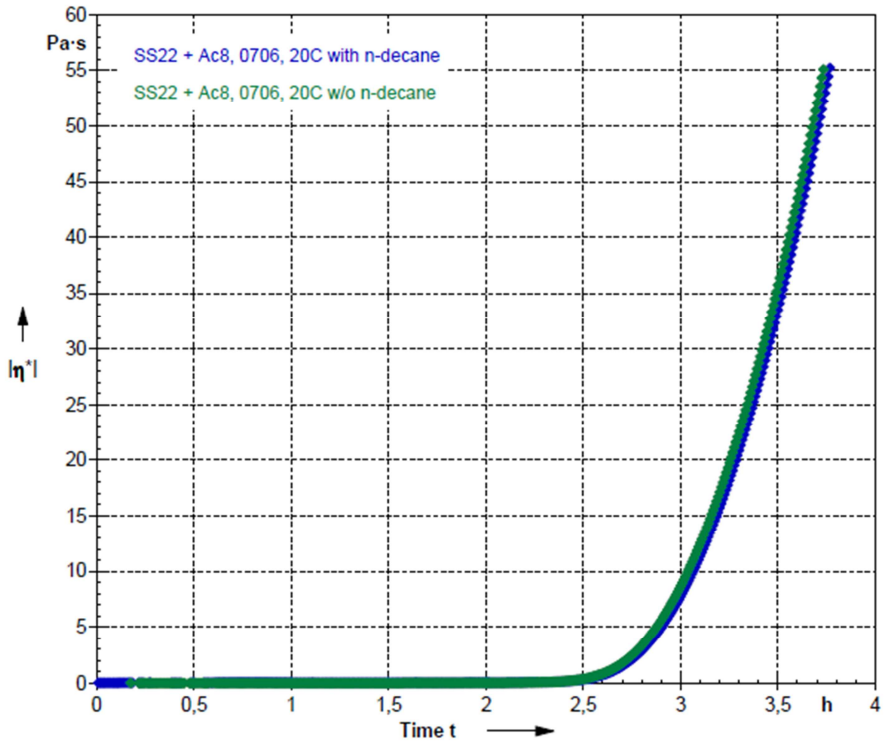

Figure 5.1. Examine the effect of n-decane on sol-gel transition time.

The sol-gel transition time of the sample without n-decane was 2.49 hrs while the corresponding one for the sample with n-decane was 2.52 hrs. The difference between two experiments was only 2 minutes, 1.83% error, which can be considered as a negligible difference considering all potential uncertainties. Moreover, the two viscosity curves presented in Fig. 5.1 are almost overlapping, which shows the behavior of the two samples is practically the same.

From these experiments, it can be concluded that the presence of n-decane has no impact on the gelation process, sol-gel transition time, and properties of the created gel, and therefore the reported results in the remaining of this work where n-decane was used to avoid water vaporization are accurate.

5.2 Effects of gel system components concentration on gel point

Test purpose

Examine the dependence of sol-gel transition time on the concentration of gel system components: sodium silicate solution and activator. And also assess the gel strength for each sample.

Gel preparation

Sodium silicate solution was weighed in a glass beaker using METTLER TOLEDO AB104-S/FACT weight scale, and then the calculated amount of activator was added to the same beaker. The final solution was then put aside for mixing on magnetic stirrer for least 5 minutes, before pouring the entire sample into the measuring cup. 1 ml of n-decane was added on the top of the sample to minimize evaporation.

Compositions of samples are presented in the Table 5.1.

Temperature setting

Temperature was set in a ramp profile, which started from 20^{o}C - ambient room temperature to 40^{o}C - designed test temperature, in the first 10 minutes of experiment. After that the temperature was kept constant at 40^{o}C.

Test procedure

Each sample was first tested under DMA mode to find the sol-gel transition time. After the gel point has achieved, the measurements were continued to observe the viscosity growth. When the viscosity has reached to a certain value, meaning the sample has reached to a certain degree of gelation, the first mode discontinued for 1 minute, and started the second mode (Amplitude sweep) to assess the gel strength at that time.

With the purpose of checking gel strength versus time, a sample with 25% of activator was chosen to run the amplitude sweep at different viscosity values after the gel point was identified. For each time, after mixture has gelled, we had to wait until the viscosity reached to a certain designed number, and then start the amplitude sweep. The constant amplitude mode was usually

run at first to have easier way on monitoring viscosity value and also to check the repeatability on gel point.

Test results and discussion

a. Determination of sol-gel transition time

Table 5.1 presents the sol-gel transition time of several samples at different component concentrations and at 40°C. In addition, the viscosity, and storage and loss moduli G' and G" at gel point are also recorded.

Table 5.1. Test results of samples at different component concentrations at 40°C

Sample	Sodium silicate solution (%)	Activator (%)	Sol-gel transition time (hrs)	G' & G" at gel point (Pa)	Viscosity at gel point (Pa·s)
1	65.0	35.0	**0.28**	1.372	0.195
2	72.8	27.2	**0.69**	2.2759	0.015
3	75.0	25.0	**0.93**	2.807	0.398
4	77.0	23.0	**1.25**	3.422	0.484
5	78.6	21.4	**1.53**	3.81	0.539
6	80.0	20.0	**2.14**	4.143	0.586
7	81.8	18.2	**2.93**	4.899	0.693
8	83.0	17.0	**3.92**	5.4399	0.769
9	84.5	15.5	**5.78**	6.021	0.852
10	86.0	14.0	**8.34**	7.218	1.021
11	86.7	13.3	**10.19**	7.8324	1.108
12	87.5	12.5	**12.30**	9.094	1.288
13	89.3	10.7	**21.45**	11.38	1.610
14	90.9	9.1	**32.79**	14.661	2.073

As we can see from the table, when the concentration of activator decreased or the concentration of sodium silicate solution increased, the mixtures took longer time to gel.

We also notice that the viscosity, storage modulus G' and loss modulus G" values of mixtures at gel points were following a trend (except the sample 2). Their values are higher at lower concentration of activator or at higher concentration of sodium silicate.

The measured results of sol-gel transition time in the dependence of activator are plotted in the Figure 5.2.

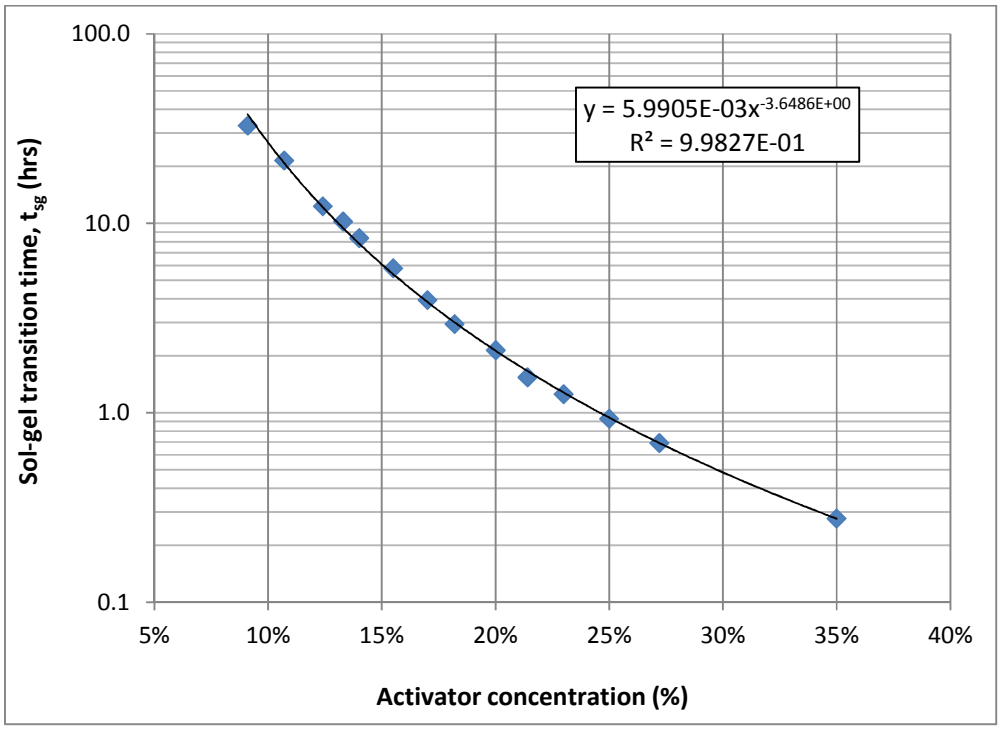

Figure 5.2. Sol-gel transition time as a function of activator concentration in a constant total weight sample.

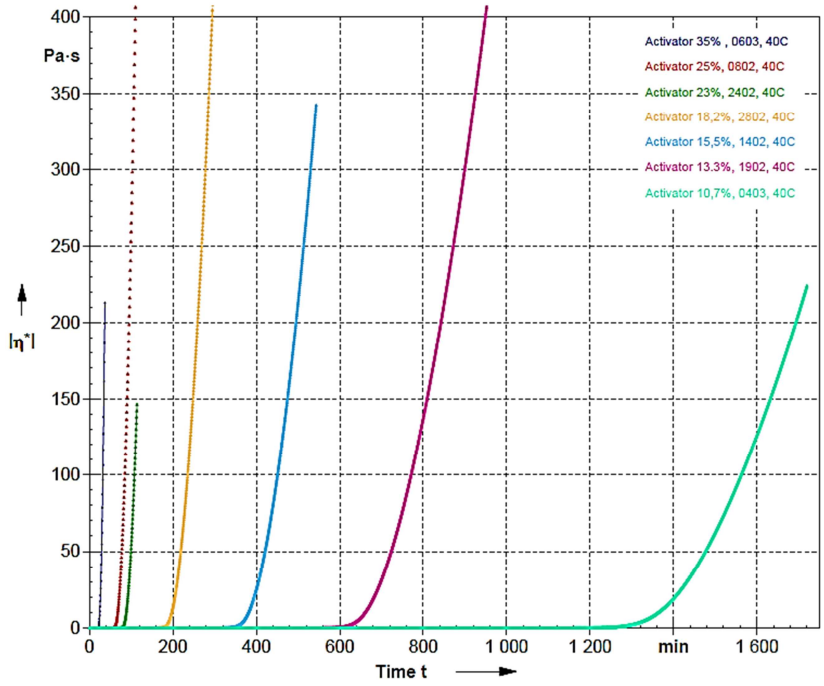

Figure 5.3. Viscosity curves of some samples at 40°C.

It might not be so clear for all the curves in the Figure 5.3 but looking at the last two viscosity curves (one with 13.3% and the other with 10.7% of activator), it can be noticed that they have different slopes. These slopes characterize the speed of viscosity growth: the higher the slope, the faster the viscosity grows.

Table 5.2. Growth of viscosity at different activator concentration

Activator, (%)	Viscosity, (Pa·s)							
	10	50	90	140	240	340	450	510
35.0%	0.07	0.14	0.19	0.23				
25.0%	0.14	0.3	0.4	0.5	0.65	0.77	0.89	
23.0%	0.16	0.34	0.46	0.57				
18.2%	0.75	1.09	0.88	1.1	1.45	1.75		
15.5%	0.51	1.17	1.58	1.99	2.66	3.19		
13.3%	0.75	1.8	2.45	3.11	4.18	5.08	5.95	6.38
10.7%	1.21	3.09	4.27	5.46				

** the table presents time in hrs for each sample with given activator concentration to reach specific viscosity after gel point*

By comparing two extreme cases, which are sample with 35% activator and sample with 10.7% activator, we can see a clear difference in the viscosity growth rate. The sample with 35% activator took only 0.23 hrs (almost 14 min) to reach to viscosity 140 Pa·s, while sample with 10.7% needed almost 5.5 hrs to reach to the same value of viscosity. In this analysis, we see again the effect of activator in acceleration of gelation process. The more activator in the sample, the faster gel structure develops.

The experiments in this section have given us some ideas and knowledge about how the gelling process is affected by the solution components concentration. However, since the concentration of sodium silicate solution and activator always changed together, we cannot derive equation to describe the relation between the sol-gel transition time with either activator or sodium silicate solution individually.

Realizing this problem, we will carry the experiments in the different way in the next sections.

b. Determination of viscoelastic properties of formed gels

The amplitude sweep mode was run in all the samples right after the DMA mode is stopped to evaluate the viscoelastic properties. At this time, each sample has reached to a certain degree of gelation with certain value of viscosity. It's difficult to set-up amplitude sweep test at the same viscosity for all samples, so then the amplitude sweep was carried at different values of viscosity, whichever we got at the time we stopped the DMA test.

An example of test result of sample with 15.5% of activator is presented below.

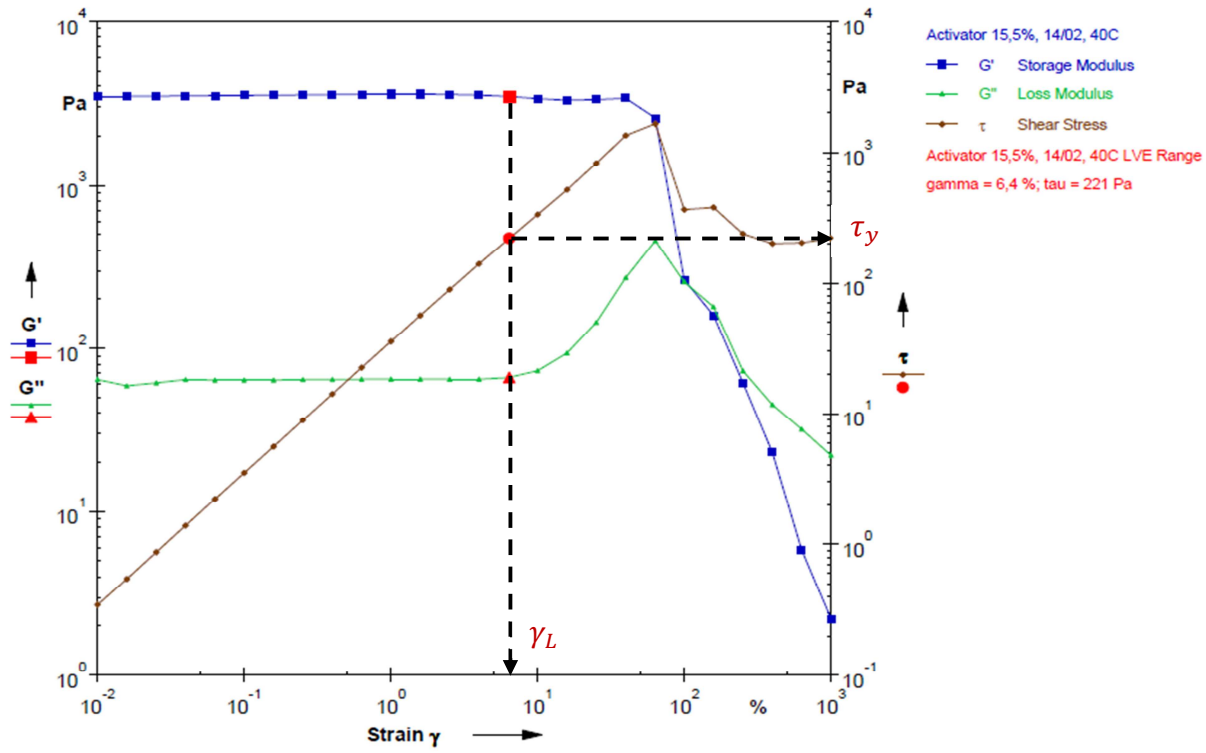

Figure 5.4. Amplitude sweep on sample with 15.5% of activator.

Limiting value of LVE range γ_L and yield stress/ yield point τ_y of this sample were detected by analysis program and they equal 6.4% and 221 Pa accordingly.

Table 5.3 presents values of limiting value of LVE range γ_L, yield stress τ_y, storage modulus G' and loss modulus G" of all samples at their tested viscosity values.

Table 5.3. Viscoelastic properties of the formed gel.

Activator (%)	Viscosity @ start of AS test (Pa.s)	Limiting value of LVE range (%)	Yield stress (Pa)	G' within LVE range (Pa)	G" within LVE range (Pa)
25.0%	510	6.62	376	5450	187
23.0%	157	5.52	102	1760	62.5
21.4%	253	7.39	206	2570	72.7
20.0%	480	7.39	374	4720	113
18.2%	154	7.71	126	1680	45.9
17.0%	369	6.52	242	3770	73.7
15.5%	346	7.84	267	3520	63.6
14.0%	828	7.1	606	8520	123
10.7%	227	5.48	117	2280	44.9
9.1%	164	2.43	39.2	1650	47.2

Results from amplitude sweep on samples with 25% of activator, at different viscosity values are presented below:

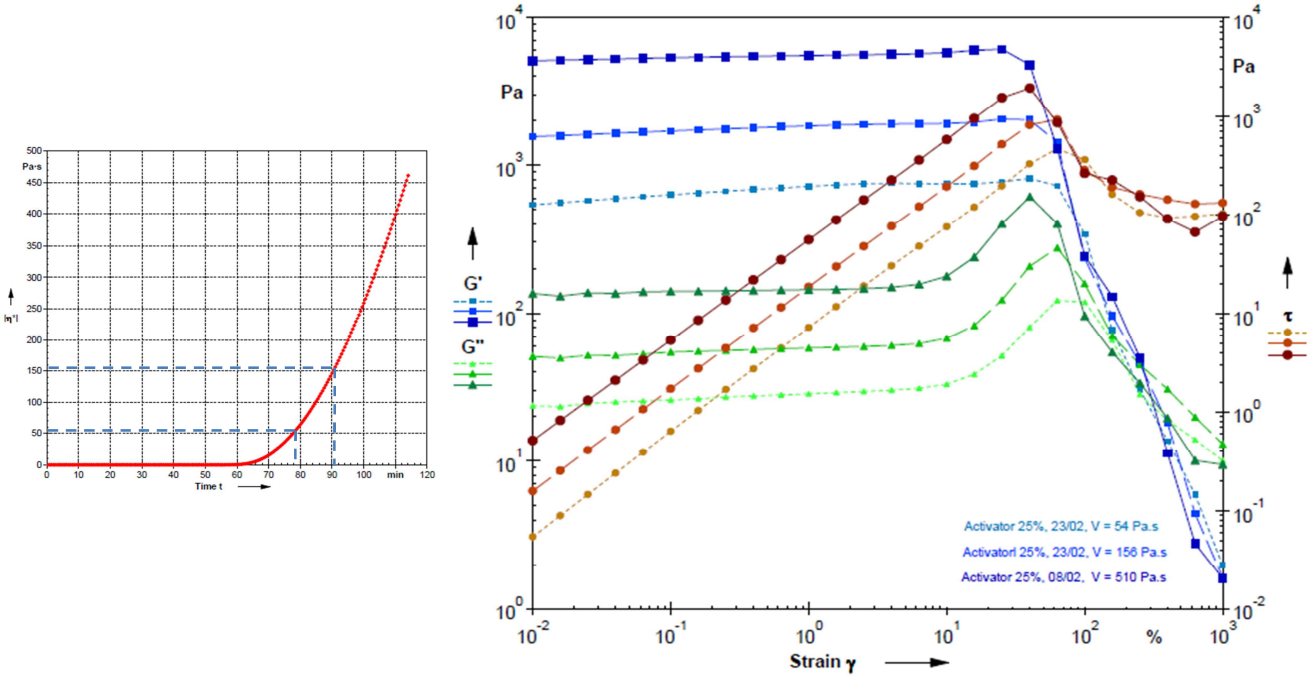

Figure 5.5. Amplitude sweep on sample with 25% of activator at different viscosity.

On the left side of the Figure 5.5, we have the viscosity curve of sample with 25% of activator, which achieved from DMA test. The two dotted lines show the viscosity values, at which the amplitude sweep was performed.

As we can see from graphs, the higher viscosity, the higher G', G" and τ the gel obtained. The higher shear stress τ, the stronger the gel will be.

5.3 Comparison and validation with literature results

Bjørn *et al.* (2011) performed a study on the same sodium silicate solution ("liquid silica") using the same activator. However, these authors used a different equipment (Brookfield PVS Rheometer) and a pressurized configuration in addition to using larger samples (>200 ml) compared to this work. The "gelation time" term was defined as the time required before the sealant starts to build viscosity. The experiments were performed at temperatures ranging from 50°C to 150°C and results are presented in Figure 5.6 below.

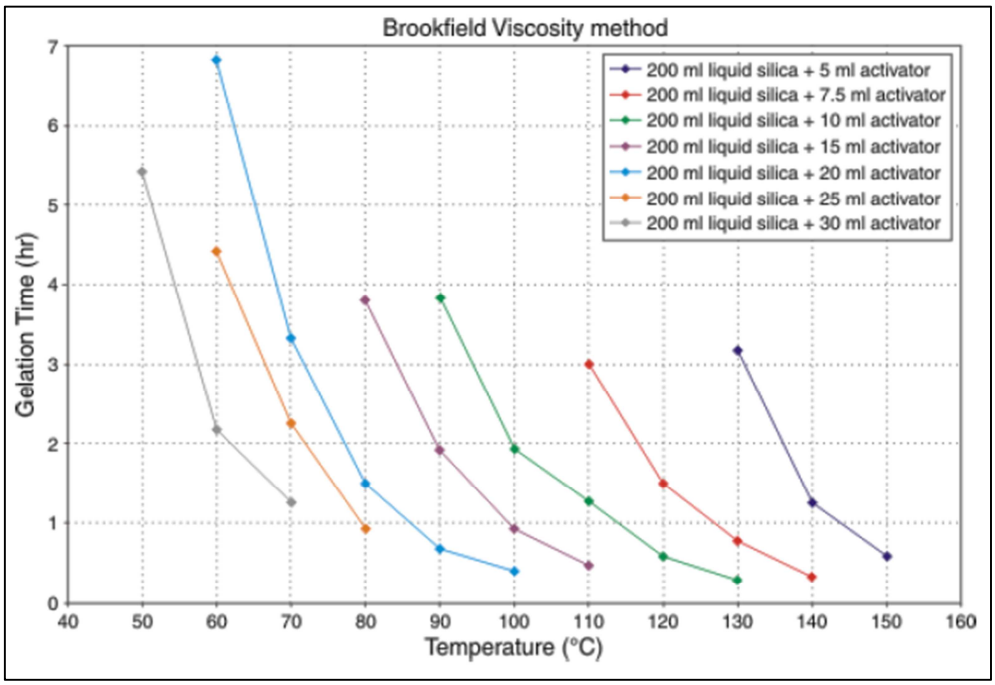

Figure 5.6. Gel-setting time from use of a Brookfield PVS Rheometer (Bjørn, et al., 2011)**.**

Test purpose

With the purpose of comparing our measurement methodology and validation with the results from Bjørn's work (2011), three samples were selected to test.

Gel preparation

Due to limited availability of the chemical and also the small required amount of sample for measurement, the total volume of mixtures were reduced by 10 times compared to the samples' volumes used by Bjørn et al. (2011); the ratio of the various components was kept the same. At this stage, together with the use of n-decane, the solvent trap was also available to further reduce sample evaporation. Distilled water was filled in the lower part of solvent trap to create a seal between upper and lower part. Water must be filled with high care to avoid water dropping to the sample.

Temperature setting

Temperature was set in a ramp profile starting from 20^{o}C - ambient room to temperature of 60^{o}C – the designed test temperature, with the increase achieved during the first 10 minutes of the experiment. After that the temperature was kept constant at 60^{o}C.

Test procedure

Three samples were tested in only DMA mode to define the sol-gel transition time.

Test results

Table 5.4 presents the comparison between results from literature and experiments done in this work.

Table 5.4. Comparison between Bjørn et al. (2011) ***gelation time and experiment results of this work.***

Sample	Components		Bjørn et al. (2011) gelation time (hrs)	Sol-gel transition time – this work (hrs)	Difference (%)
	Sodium silicate solution (ml)	Activator (ml)			
1	20	3	2.15	2.6	20.9%
2	20	2.5	4.4	5.73	30.27%
3	20	2	6.8	8.79	29.3%

Our sol-gel transition time is always longer than gelation time from Bjørn *et al.* (2011) gelation time results. The differences are large; however they are quite in the same range. The reason for this deviation could be explained by:

- ***The difference in used equipment's***. It's obviously that with pressurized configuration in Bjørn et al. (2011) work, the samples exposure to a more homogeneous temperature environment. Since the pressurized configuration is a seal closed system during measurement, the heat loss is less in compare with the bob/cup system in this work. That's could be the reason that makes the gelation happened earlier.
- ***The difference in nature of reported points.*** Bjørn et al. (2011) might have used a certain degree of gelation as a reference and reported the gelation time when the samples reached that degree. And this degree of gelation could be different with the one used in this work.

5.4 Effect of activator concentration on sol-gel transition time

Test purpose

Because of the mentioned issue at the end of section 5.2, we should carry the experiments in the way, which enable us to derive the function between sol-gel transition time and one component only. In this section, we will keep concentration of sodium silicate constant while varying concentration of activator. In order to do that, water need to be added to the sample. Distilled water was used for these experiments, so it can be sure that there are no effects from other ions on sol-gel transition.

Gel preparation

In these experiments, the concentration of sodium silicate solution in the sample was kept constant at 80 wt%, while the concentration of the activator and distilled water were varied. The total weight of gel solution was designed to be fixed at 30 g.

Sodium silicate solution was weighed in a glass beaker, and then the calculated amount of distilled water and activator were added to the same beaker sequentially. The final solution was then put aside for mixing using a magnetic stirrer for least 5 minutes, before placing it into the measuring cup. A solvent trap and n-decane were used as measures to reduce evaporation.

Temperature setting

Temperature was set in the same way as in section 5.2. Test temperature was 40^{o}C.

Test procedure

All the samples were tested in 2 modes as in section 5.2.

Test results and discussion

a. Sol-gel transition time

Experiment results are presented in Table 5.5 and sol-gel transition time is plotted vs. activator weight concentration in Figure 5.7.

Table 5.5. Effect of activator on sol-gel transition time.

Sample	Total sample weight (g)	Sodium silicate system (g)	Activator (g)	DW (g)	Activator (%)	Sol-gel transition time (hrs)	G' & G" at gel point (Pa)	Viscosity at gel point (Pa.s)
1	30	24	6	0	**20.00%**	**2.69**	0.60519	4.2786
2			5	1	**16.67%**	**6.22**	0.7401	5.2332
3			4.5	1.5	**15.00%**	**9.93**	0.84313	5.9618
4			4	2	**13.33%**	**18.32**	0.92802	6.5621
5			3.5	2.5	**11.67%**	**33.60**	1.1427	8.0802

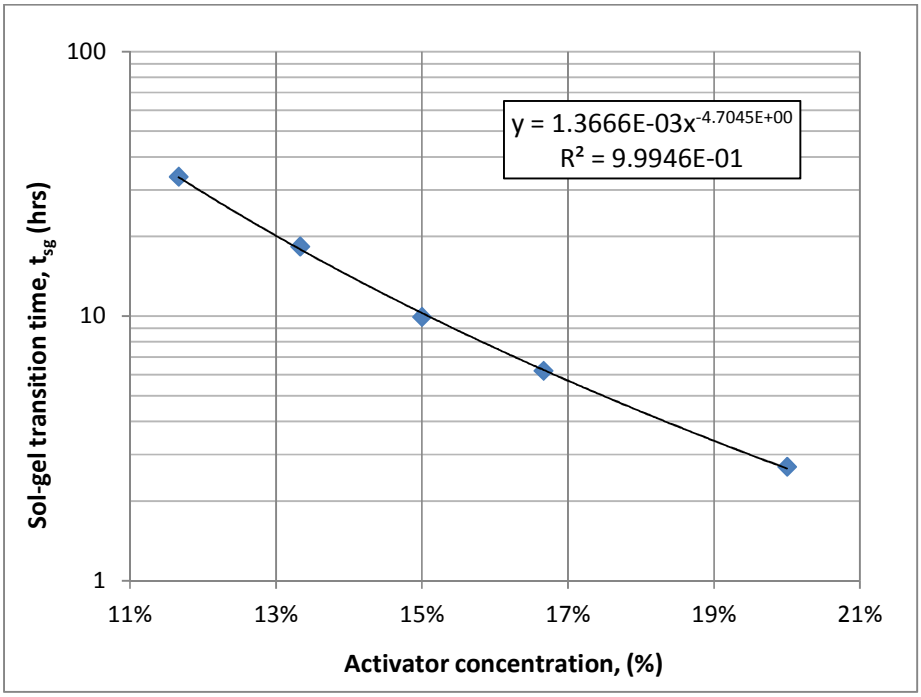

Figure 5.7. Sol-gel transition time vs. activator weight concentration.

A power function was chosen that best-fitted the measured data and the resulting expression is $y = 1.3666 \cdot 10^{-3} \cdot x^{-4.7045}$, where y is sol-gel transition time and x is activator concentration. Since the power regression type described the relation better than the exponential type, so then, the equation (xx) will be replaced by:

$$t_{sg} = 1.3666 \cdot 10^{-3} \cdot [Ac]^{-4.7045} \qquad (Ac - Activator)$$

This equation is valid for solution with 80% of sodium silicate solution.

As we can see from the graph, the sample with higher activator concentration, the faster it gels.

b. Viscoelastic properties of formed gels

Table 5.6 presents values of limiting value of LVE range, yield stress, storage modulus and loss modulus of all samples at their tested viscosity values.

Table 5.6. Viscoelastic properties of the formed gel.

Sample	Sodium silicate system (%)	Viscosity @ start of AS test (Pa.s)	Limiting value of LVE range (%)	Yield stress (Pa)	G' within LVE range (Pa)	G" within LVE range (Pa)
1	86.67%	529	6.77	351	5280	78.8
2	83.33%	366	6.94	242	3640	55.2
3	80.00%	376	6.9	252	3790	53.9
4	76.67%	2400	4.07	978	23949	283.4
5	70.00%	2.92	16.1	3.64	27.1	9.74

5.5 Effect of sodium silicate concentration on sol-gel transition time

Test purpose

In this section, the effect of sodium silicate concentration on sol-gel transition time is examined with the activator concentration kept constant while the silicate and distilled water concentrations in the total sample are varied accordingly; the total weight of the sample is kept constant at 30 g.

The sample number 4 from Table 5.5, which contains 24 g of sodium silicate solution, 4 g of activator and 2 g of distilled water, was chosen to be the base case experiment in this section. The activator concentration was kept constant at 13.33%.

Gel preparation

Gel preparation was carried on the same procedure as in section 5.4.

Temperature setting & Test procedure

The same way was performed as in section 5.2. Test temperature was 40^{o}C.

Test results and discussion

a. Sol-gel transition time

Experiment results are presented in Table 5.7 and sol-gel transition time is plotted vs. concentration of sodium silicate solution in Figure 5.8.

Table 5.7. Effect of sodium silicate solution on sol-gel transition time.

Sample	Total sample weight (g)	Sodium silicate system (g)	Activator (g)	DW (g)	Sodium silicate system (%)	Sol-gel transition time (hrs)	G' & G" at gel point (Pa)	Viscosity at gel point (Pa.s)
1	30	26	4	0	**86.67%**	**14.13**	1.1357	8.0308
2		25		1	**83.33%**	**16.23**	1.0459	7.3957
3		24		2	**80.00%**	**18.32**	0.92802	6.5621
4		23		3	**76.67%**	**20.80**	0.8753	6.1893
5		21		5	**70.00%**	**30.41**	0.57099	4.0375

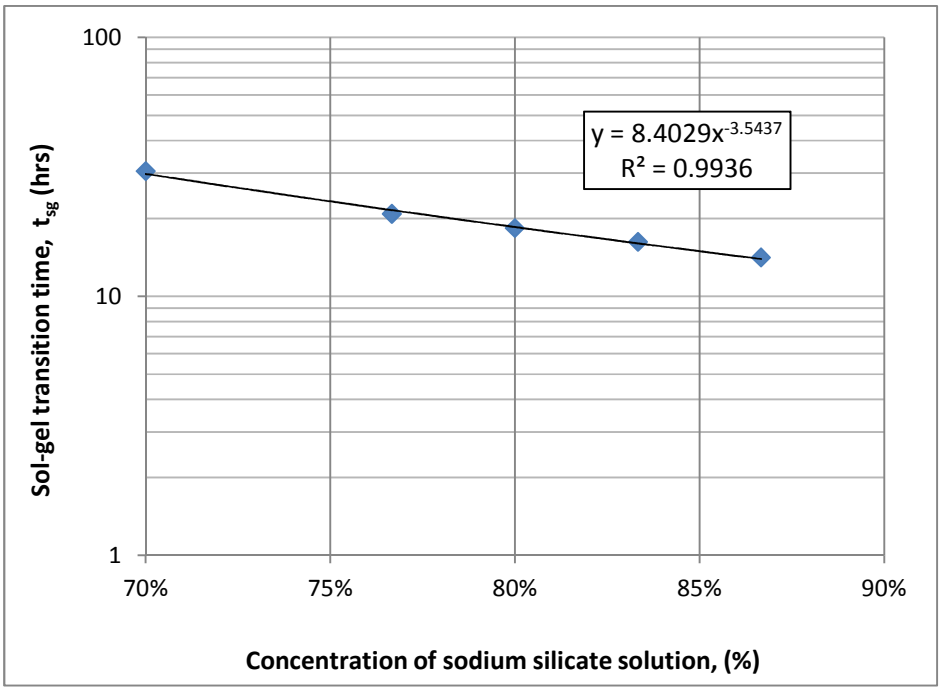

Figure 5.8. Sol-gel transition time versus weight concentration of sodium silicate solution.

Among the Trend/Regression Type, again the power function fitted the best to measured points and its equation is $y = 8.4029 \cdot x^{-3.5437}$, where y is sol-gel transition time and x is concentration of sodium silicate solution in the sample. Since the power regression type described the relation better than the exponential type, so then, the equation (xx) will be replaced by:

$$t_{sg} = 8.4029 \cdot [SS]^{-3.5437} \qquad (SS - sodium\ silicate\ solution)$$

This equation is valid for solution with 13.33% of activator.

From experiments in this section, we see the similar effect as with activator on sol-gel transition time in a way that, the higher concentration of silicate, the shorter sol-gel transition time sample required. However, it seems that the activator had a higher effect on sol-gel transition time than silicate. In order to see it clearly, we will compare the effect of these two components in next sub-section.

b. Viscoelastic properties of formed gels

Table 5.8 presents values of limiting value of LVE range, yield stress, storage modulus and loss modulus of all samples at their tested viscosity values.

Table 5.8. Viscoelastic properties of the formed gel.

Sample	Activator (%)	Viscosity @ start of AS test (Pa.s)	Limiting value of LVE range (%)	Yield stress (Pa)	G' within LVE range (Pa)	G" within LVE range (Pa)
1	20.00%	108	6.23	70.4	1129	33.3
2	16.67%	54.6	4.01	22.7	571.8	23.1
3	15.00%	286	7.65	211	2890	49.6
4	13.33%	53	3.51	18.1	535.4	22.9
5	11.67%	33.1	3.6	11.3	334.3	26.4

5.5.1 Comparison between activator and sodium silicate effects on sol-gel transition

In order to compare the effects of activator and sodium silicate on the sol-gel transition time, the experimental results from sections 5.4 and 5.5 are plotted together as shown in Figure 5.9 below. The blue line indicates the relationship between sol-gel transition times with concentration of activator at constant concentration of sodium silicate solution equals 80%, and the red line indicates the relationship between sol-gel transition times with concentration of sodium silicate solution at constant activator concentration equals 13.33%.

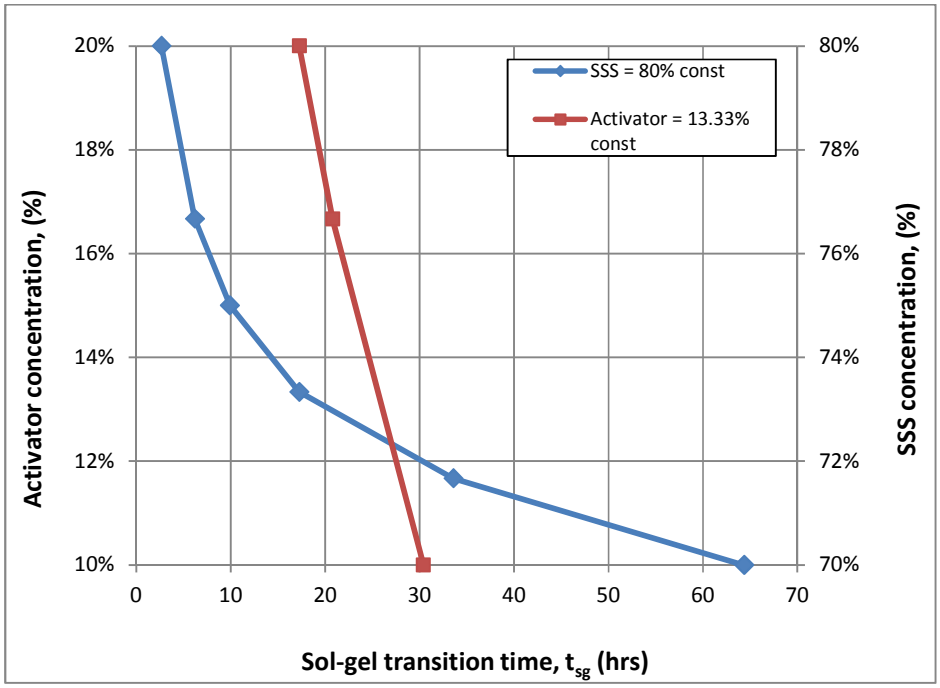

Figure 5.9. Sol-gel transition time versus activator and sodium silicate solution concentration.

Figure 5.9 shows that the gel formation rate is more sensitive to the change of the activator concentration than the silicate concentration. For example, an increase by 10% of the activator concentration (from 10% to 20%) decreased the sol-gel transition time of the examined sample from the original 64.37 hrs down to 2.69 hrs – almost 62 hrs difference. Meanwhile, with a 10% increase of the sodium silicate solution concentration (from 70% to 80%) reduced the sol-gel transition time from 30.41 hrs to 17.27 hrs – only around 13 hrs difference.

5.5.2 Comparison between silicate gel and polymer gel system in term of viscosity growth

In order to compare the viscosity growth between silicate gel and polymer gel system, some works on polymers has been reviewed. The polymer viscosity curves, which are presented on the left side of Figure 5.10, are achieved from work done by Sydansk (1990). The viscosity curve of silicate gel, which is presented on the right side of Figure 5.10, is achieved when testing the sample with 24 g of sodium silicate solution and 6 g of activator at 60°C.

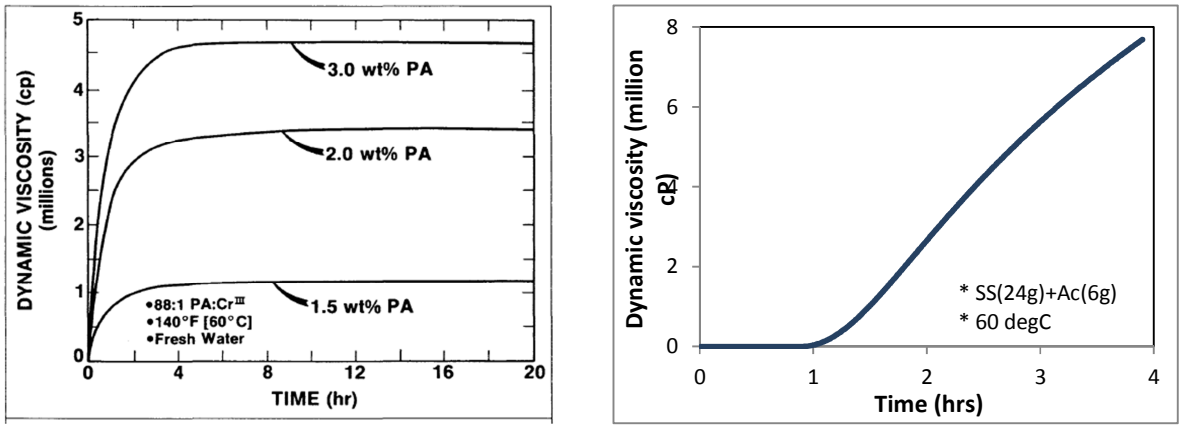

Polymer Silicate gel

Figure 5.10. Viscosity growth of polymer vs. silicate gel system.

From Figure 5.10, it is clear that polymer and silicate gel have different mechanism for viscosity growth.

Polymer:

- Rapid change, the viscosity starts to increase right after adding cross-linker.
- Viscosity reaches to almost constant value at the end of gelling process.

Silicate gel:

- Slow change, it takes certain time (in the dependence of gel composition) for viscosity to start a sharp increase.

- Viscosity rate keeps increasing until it reaches to a constant rate, which is expressed in a constant slope.
- After sometimes, the growth rate decreases slightly (slope reduced).

5.6 Temperature effects

This work is aimed to design a water shutoff treatment at an injection well in a naturally fractured formation using the silicate gel system under investigation. The effective distance of the formed gel in the formation is designed to be half way between the injection and the production well. The temperature at production well is around 60^{o}C and the temperature at injection well is around 40^{o}C (temperature is cooled down due to continuous water injection). Therefore, the silicate system pumped into formation will be exposed to various temperatures which may affect its gelation time. In order to examine this temperature dependency of the silicate system the tests were conducted at temperatures of 40^{o}C, 45^{o}C, 50^{o}C, 55^{o}C and 60^{o}C.

From literature review of previous related works, we know that temperature accelerates the gelation process (Stavland *et al*. (2011), Bjørn *et al*. (2011)), i.e., the higher the temperature, the faster the gel will be formed. This effect should also be included in the unified sol-gel transition time correlation.

A sample with 24 g of sodium silicate solution, 6 g of activator and 2.5 g of distilled water was chosen to test the gelation process at temperatures of 40^{o}C, 45^{o}C, 50^{o}C, 55^{o}C and 60^{o}C.

Temperature setting

Temperature was set in a two linear ramp profiles to increase the temperature from room temperature 20^{o}C to desired test temperature (45^{o}C, 50^{o}C, 55^{o}C and 60^{o}C) and followed by a constant temperature profile of desired test temperature:

- First linear ramp profile: increase temperature from 20^{o}C to 40^{o}C in 10 minutes.
- Second linear ramp profile: increase temperature from 40^{o}C to desired test temperature 45^{o}C, 50^{o}C, 55^{o}C and 60^{o}C in 2.5; 5; 7.5; 10 minutes, respectively.
- Third constant temperature profile: temperature is kept constant at desired test value.

Test procedure

All samples were tested at both test modes as described above.

Test results and discussion

The sol-gel transition times of the sample with 24 g of sodium silicate solution, 6 g of activator and 2.5 g of distilled water at different temperatures are presented in the table below:

Table 5.9. Sol-gel transition time at various temperatures.

Temperature		1/T, (1/K)	Sol-gel transition time, (hrs)	Viscosity @ gel point, (Pa.s)	G' &G" @ gel point, (Pa)
°C	°K				
40	313.15	0.003193	**5.09**	0.52578	3.7176
45	318.15	0.003143	**3.76**	0.48283	3.4140
50	323.15	0.003095	**2.68**	0.46465	3.2844
55	328.15	0.003047	**1.91**	0.43169	3.0508
60	333.15	0.003002	**1.43**	0.42001	2.9644

The temperature effects significantly on sol-gel transition time. The temperature increase of 10^{o}C shortened the sol-gel transition time almost 2 times. It also effected on gelation rate, which can be seen on slope of viscosity curves on Figure 5.11.

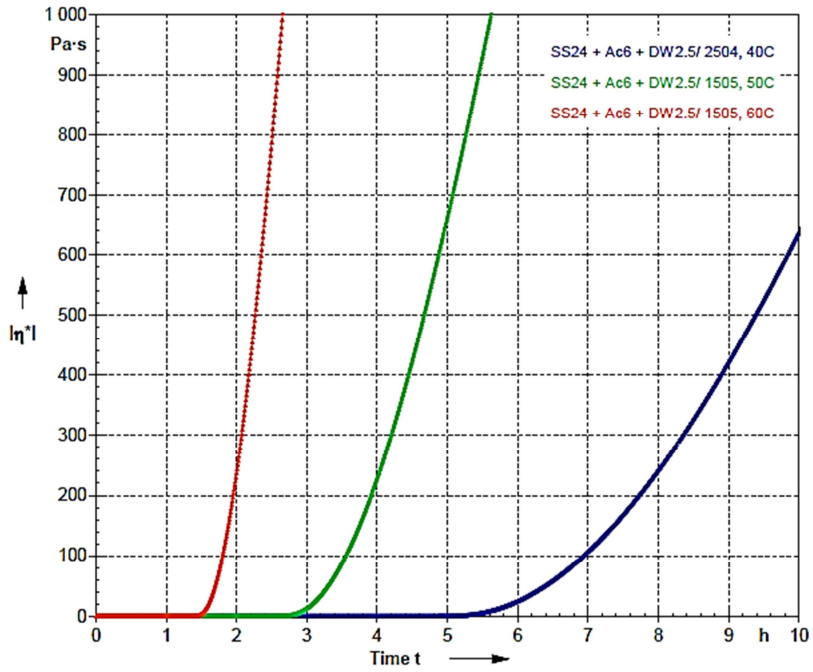

Figure 5.11. Viscosity growth at different temperatures.

The sol-gel transition times are plotted versus the inverse absolute temperature in Figure 5.12.

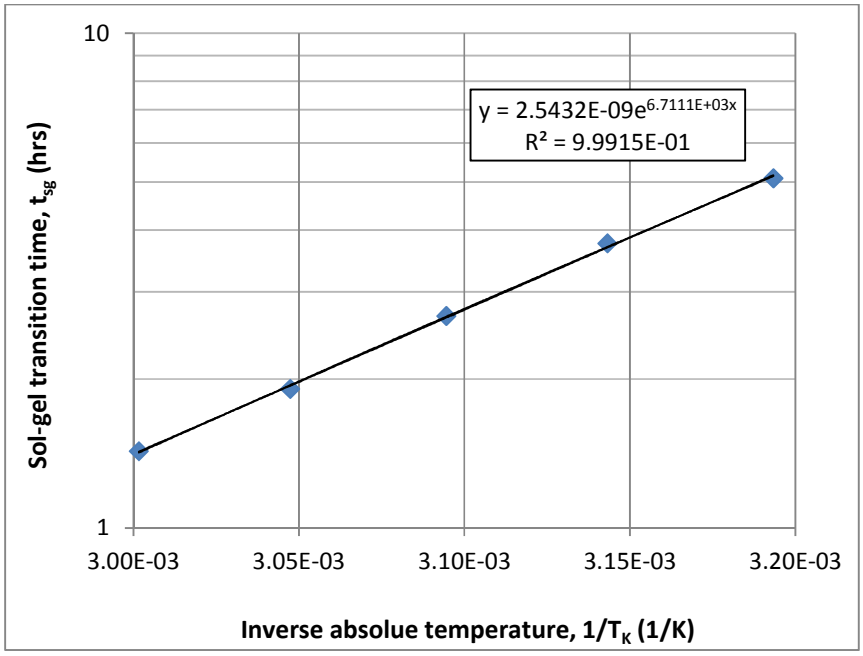

Figure 5.12. Sol-gel transition time vs. inverse absolute temperature.

The relation between sol-gel transition time and inverse of absolute temperature is best described by the exponential function, which is also can be written in the form of Arrhenius' equation as follows:

$$t_{sg} = \xi \times e^{E_a/RT_K} = 2.5432 \times 10^{-9} \times e^{6711.1x}.$$

Since $x = 1/T_K$, then $E_a/R = 6711.1$, then the activator energy used in this work is:

$$E_a = 6711.1 \times 8.314 \times 10^{-3} = 55.8 \text{ kJ/mol}.$$

The function, which describes the effect of temperature, can be written again as follows:

$$t_{sg} = 2.543 \times 10^{-8} \times e^{\frac{6711.1}{T_K}}.$$

5.7 Divalent ion effect

On the way from surface to final destination in the formation, the silicate gel system will meet with injected and formation water, which contain divalent ions Ca^{2+} and Mg^{2+}. These ions have some effects on gel system, specifically on sol-gel transition time. At high concentration, they might even cause precipitation of calcium or magnesium silicate. There will be a need of pre-flush in that case before injecting the silicate gel solution. Results from the following tests will show how sol-gel transition time is affected by a presence Ca^{2+} or Mg^{2+} separately.

5.7.1 Effect of ion Ca^{2+}

Gel preparation

Before preparing sodium silicate samples for this experiment, distilled water with various concentrations of calcium ion Ca^{2+} such as 100, 300, 500, 750 and 1000 ppm was made up in separate bottles, using calcium chloride dehydrate $CaCl_2.2H_2O$.

After that, 30 g of each sample was made up from 24 g of sodium silicate solution, 6 g of activator and 2.5 g of distilled water, which contained the desired concentrations of calcium ion Ca^{2+}.

Starting with 24 g of sodium silicate solution, then adding 6 g of activator, and finally 2.5 g of distilled water with the desired concentration of Ca^{2+} were added into a glass beaker sequentially. The final solution was then put aside for mixing using a magnetic stirrer for least 5 minutes, before placing it into the measuring cup of Rheometer. As mentioned previously, a 1 ml layer of n-decane was added on the top of all samples and the addition of solvent trap was used as measures to reduce vaporization effects.

Temperature setting

The testing temperatures were 40^{o}C, 50^{o}C and 60^{o}C. They are set in the same way as described in section 5.6.

Test procedure

All the samples were tested in 2 modes as described in section 5.2.

Test results and discussion

a. <u>Sol-gel transition time</u>

Experiment results are presented in Table 5.10 and sol-gel transition time is plotted vs. activator weight concentration in Figure 5.13.

Table 5.10. Sol-gel transition time at various Ca^{2+} concentration and temperature.

T, (°C)	Sample	Total sample weight (g)	Sodium silicate solution (g)	Activator (g)	DW (%)	Ca^{2+} in DW, (ppm)	Ca^{2+} in total sample, (ppm)	Sol-gel transition time (hrs)	G' & G" at gel point (Pa)	Viscosity at gel point (Pa.s)
40	1	32.5	73.85%	18.46%	7.69%	0	**0**	**5.09**	0.52578	3.7176
	2					100	**7.69**	**4.91**	0.53181	3.7603
	3					300	**23.08**	**4.36**	0.52287	3.6972
	4					500	**38.46**	**3.94**	0.51302	3.6273
	5					750	**57.69**	**3.43**	0.49673	3.5123
	6					1000	**76.92**	**3.07**	0.49199	3.4787
50	1					0	**0**	**2.68**	0.46465	3.2844
	2					100	**7.69**	**2.52**	0.46905	3.3156
	3					300	**23.08**	**2.23**	0.46124	3.2598
	4					500	**38.46**	**2.08**	0.46102	3.2587
	5					1000	**76.92**	**1.57**	0.46184	3.2622
60	1					0	**0**	**1.43**	0.42001	2.9644
	2					100	**7.69**	**1.34**	0.43925	3.099
	3					300	**23.08**	**1.23**	0.42883	3.0242
	4					500	**38.46**	**1.13**	0.44433	3.139
	5					1000	**76.92**	**0.92**	0.46293	3.2647

**the concentration of ion Ca^{2+} in distilled water was converted into the concentration of Ca^{2+} in total weight of sample (30g) and the last value was used to plot versus sol-gel transition time in Fig.5.13.*

As we can see from Table 5.10, the higher Ca^{2+} concentration, the shorter sol-gel transition time. The temperature also accelerates the gelation process in this case.

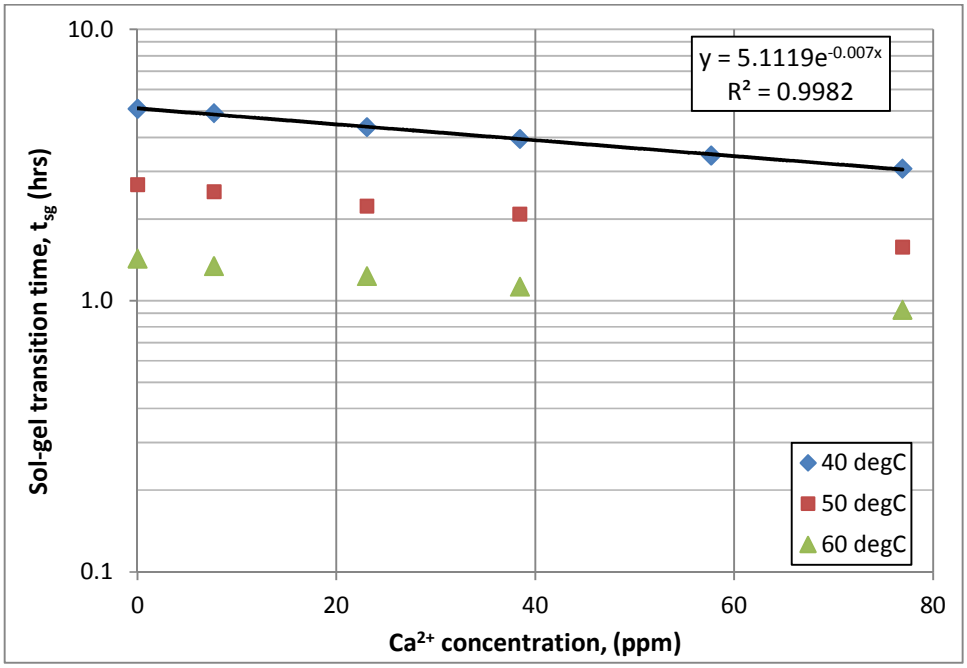

Figure 5.13. Effect Ca^{2+} on the sol-gel transition time.

The relation between sol-gel transition time and Ca^{2+} ion at 40°C is best described by an exponential function as follows:

$$t_{sg} = 5.1119 \times e^{-0.007[Ca^{2+}]}.$$

This equation will be used to build the unified sol-gel transition time correlation (3.7), while the test results at 50°C and 60°C will be used to check how accurate the estimation of sol-gel transition time at higher temperatures, using the general equation; thus finding the coefficient and develop the general equation for higher temperatures.

b. Viscoelastic properties of formed gels

Table 5.11 presents values of limiting value of LVE range, yield stress, storage modulus and loss modulus of all samples at their tested viscosity values.

Table 5.11. Viscoelastic properties of the formed gel at the presence of ion Ca^{2+}.

T, (^{o}C)	Sample	Ca^{2+} in total sample, (ppm)	Viscosity @ start of AS test (Pa.s)	Limiting value of LVE range (%)	Yield stress (Pa)	G' within LVE range (Pa)	G" within LVE range (Pa)
40	1	**0**	4040	1.64	674	40694	575.2
	2	**7.69**	1900	4.09	775	18897	297.9
	3	**23.08**	1430	4.72	684	14354	240.6
	4	**38.46**	2390	3.99	968	24024	386.1
	6	**76.92**	2560	3.27	850	25809	427.2
50	1	**0**	1210	2	246	12221	275.8
	2	**7.69**	3870	3.03	1180	38819	748.7
	3	**23.08**	2010	5.63	1170	20365	441.1
	4	**38.46**	2140	3.3	723	21631	474.2
	5	**76.92**	2950	3.27	988	29869	651.6
60	1	**0**	1720	5.57	1010	17605	503.1
	2	**7.69**	4030	4.06	1670	40526	1030.2
	3	**23.08**	4170	4.52	1790	41723	1085.5
	4	**38.46**	3120	2.37	765	31773	877.7
	5	**76.92**	2300	4.73	1180	23941	727.3

The results from Table 5.11 are plotted in the Figures below.

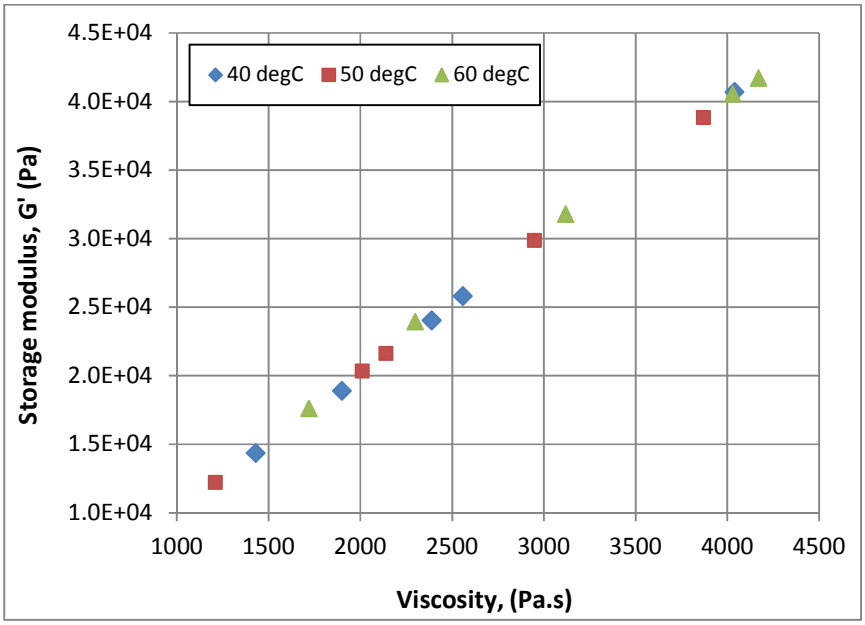

Figure 5.14. Viscosity vs. storage modulus of formed gel in the presence of ion Ca^{2+}.

Fig 5.14 shows that the storage modulus is in linear relationship with the system viscosity and that it does not depend on temperature. Increasing the viscosity leads to an increased storage modulus.

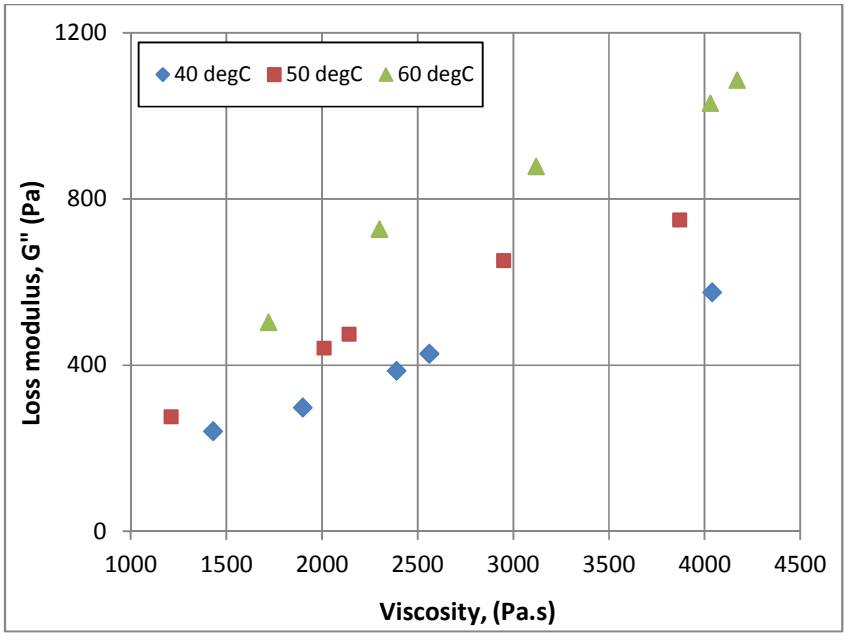

Figure 5.15.Viscosity vs. loss modulus of formed gel in the presence of ion Ca^{2+}.

Figure 5.15 shows that, the loss modulus is a function of both system viscosity and temperature. Apparently, at the same viscosity value, if the temperature is higher, then the G" is higher.

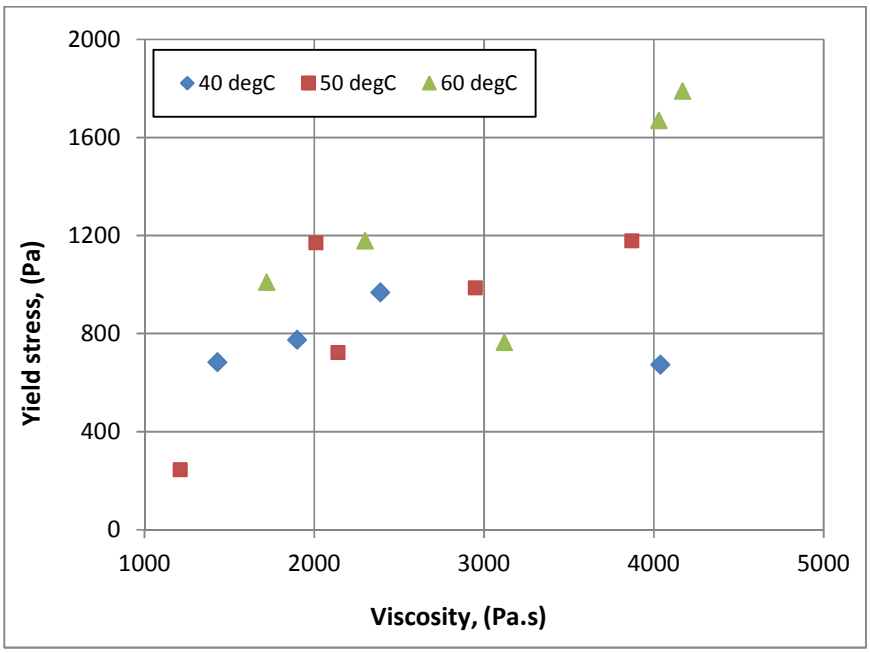

Figure 5.16. Viscosity vs. yield stress of formed gel in the presence of ion Ca^{2+}.

Figure 5.16 does not show a clear relationship between yield stress and viscosity. However, despite some out-of-trend points, it seems that at higher viscosities, the formed gels have higher yield stresses. However, as the system viscosity increases further (last blue diamond point), the gel most likely became brittle, thus leading to lower yield stresses.

5.7.1 Effect of ion Mg^{2+}

Gel preparation

Similarly with the experiments with calcium ion, before making samples for experiment, distilled water with various concentrations of calcium ion Mg^{2+} such as 100, 300, 500 and 750 ppm was made up in separate bottles, using magnesium chloride dehydrate $MgCl_2.6H_2O$.

After that, 30 g of each sample was made up from 24 g of sodium silicate solution, 6 g of activator and 2.5 g of distilled water, which contained desired concentrations of calcium ion Mg^{2+} in the same manner as in the experiments with Ca^{2+} ion.

Temperature setting

The testing temperatures were 40°C and 60°C. They are set in the same way as described in section 5.6.

Test procedure

All the samples were tested in 2 modes as described in section 5.2.

Test results and discussion

a. Sol-gel transition time

Experiment results are presented in Table 5.12 and sol-gel transition time is plotted vs. activator weight concentration in Figure 5.17.

Table 5.12. Sol-gel transition time at various Mg^{2+} concentration and temperature.

T, (°C)	Sample	Total sample weight (g)	Sodium silicate solution (g)	Activator (g)	DW (%)	Mg^{2+} in DW, (ppm)	Mg^{2+} in total sample, (ppm)	Sol-gel transition time (hrs)	G' & G" at gel point (Pa)	Viscosity at gel point (Pa.s)
40	1	32.5	73.85%	18.46%	7.69%	0	**0**	**5.09**	0.52578	3.7176
	2					100	**7.69**	**4.88**	0.51603	3.6486
	3					300	**23.08**	**4.08**	0.51095	3.6125
	4					500	**38.46**	**3.17**	0.5081	3.5923
	5					750	**57.69**	**2.19**	0.49464	3.4965
60	1					0	**0**	**1.43**	0.42001	2.9644
	2					300	**23.08**	**1.13**	0.44872	3.1677
	3					500	**38.46**	**0.93**	0.47325	3.3433
	4					750	**57.69**	**0.69**	0.45979	3.2434

As we can see from Table 5.12, the higher Mg^{2+} concentration, the shorter sol-gel transition time. The temperature also accelerates the gelation process in this case.

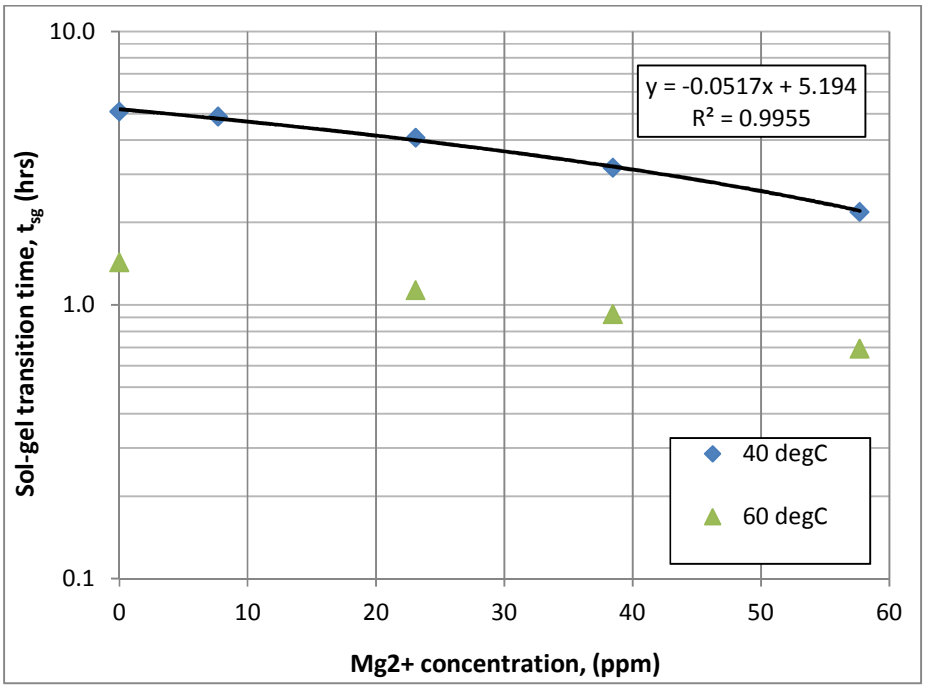

Figure 5.17. Effect of Mg^{2+} ion on sol-gel transition time.

The relation between sol-gel transition time and Mg^{2+} ion at 40°C is best described by the linear function, which is not the same form as with the ion Ca^{2+}, as follows:

$$t_{sg} = -0.0517 \times [Mg^{2+}] + 5.194.$$

This equation will be used to build the unified sol-gel transition time correlation (3.7), while the test results at 60°C will be used to check how accurate the estimation of sol-gel transition time at higher temperature, using unified sol-gel transition time correlation; thus finding the coefficient and develop the unified sol-gel transition time correlation for higher temperatures.

The difference in resulting functions, which describe the relationship between sol-gel transition time and divalent ion Ca^{2+} and Mg^{2+} could be due to the higher potential of Mg^{2+} in causing precipitation in the solution than Ca^{2+}. This phenomenon was noticed during mixing the samples. While ion Ca^{2+} at its highest concentration of 1000 ppm in distilled water (or 76.92 ppm in total sample), only made the sample turned into a slight opaque state, the presence of 38.46 ppm Mg^{2+}

in sample already created some precipitation. Figure 5.18 below shows two samples: one contains ion Ca^{2+} and the other only Mg^{2+}, but at the same concentration 76.92 ppm.

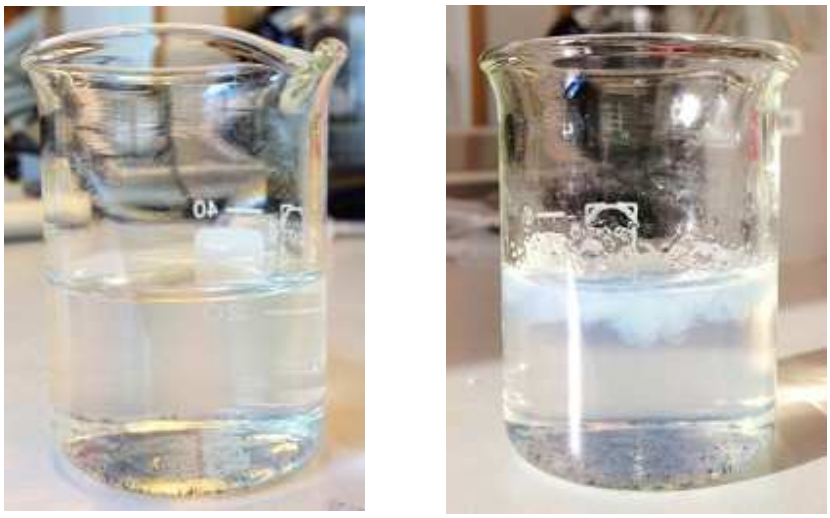

a b

Figure 5.18. Silicate gel system in contact with divalent ions: a. Ca^{2+}; b. Mg^{2+}.

It is clearly seen that Mg^{2+} resulted to a white precipitant which flows at the top of the sample (see Figure 5.18.b). The black particles seen at the bottom of the glass beakers in both samples are additives originated from the sodium silicate solution.

The injected sodium silicate system will meet with injected water that exists in the formation and will be diluted. The dilution will reduce the concentration of two main components of the gel system, which are sodium silicate solution and activator, thus will affect the sol-gel transition time.

In this section, experiments will be carried in a way to stimulate this situation, in which the injected gel system (sodium silicate solution and activator) will be mixed with distilled water in increased manner of quantity.

b. Viscoelastic properties of formed gels

Table 5.13 presents values of limiting value of LVE range, yield stress, storage modulus and loss modulus of all samples at their tested viscosity values.

Table 5.13. Viscoelastic properties of the formed gel at the presence of ion Mg^{2+}.

T, (^{o}C)	Sample	Mg^{2+} in total sample, (ppm)	Viscosity @ start of AS test (Pa.s)	Limiting value of LVE range (%)	Yield stress (Pa)	G' within LVE range (Pa)	G" within LVE range (Pa)
40	1	**0**	4040	1.64	674	40694	575.2
	2	**7.69**	1450	4.65	691	14674	242
	3	**23.08**	1100	6.04	681	11119	194.7
	4	**38.46**	872	5.06	445	8739.1	165.1
60	1	**0**	1720	5.57	1010	17605	503.1
	2	**23.08**	2480	3.07	788	25133	714.2
	3	**38.46**	2770	4.41	1280	28312	820.6

Data from Table 5.13 are also plotted in the Figures below.

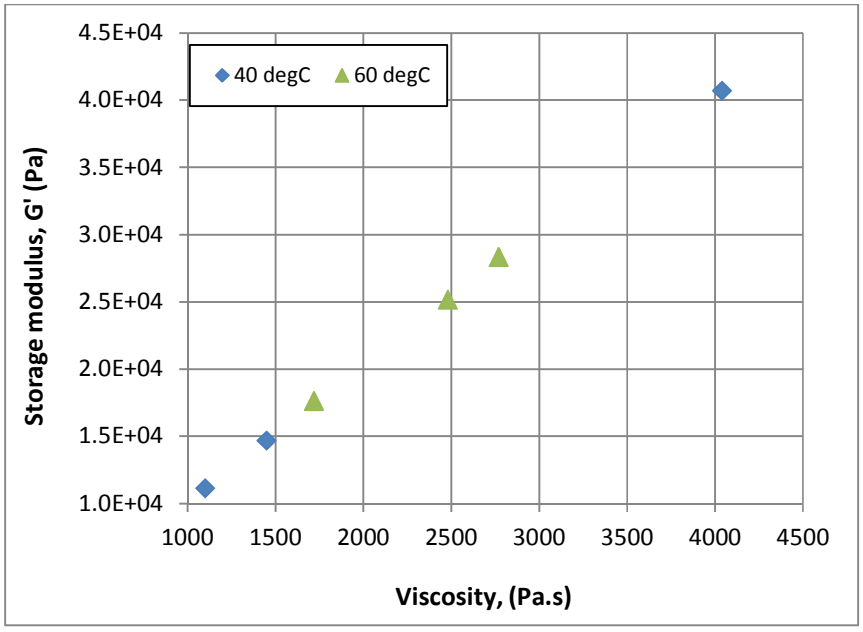

Figure 5.19. Viscosity vs. storage modulus of formed gel in the presence of ion Mg^{2+}.

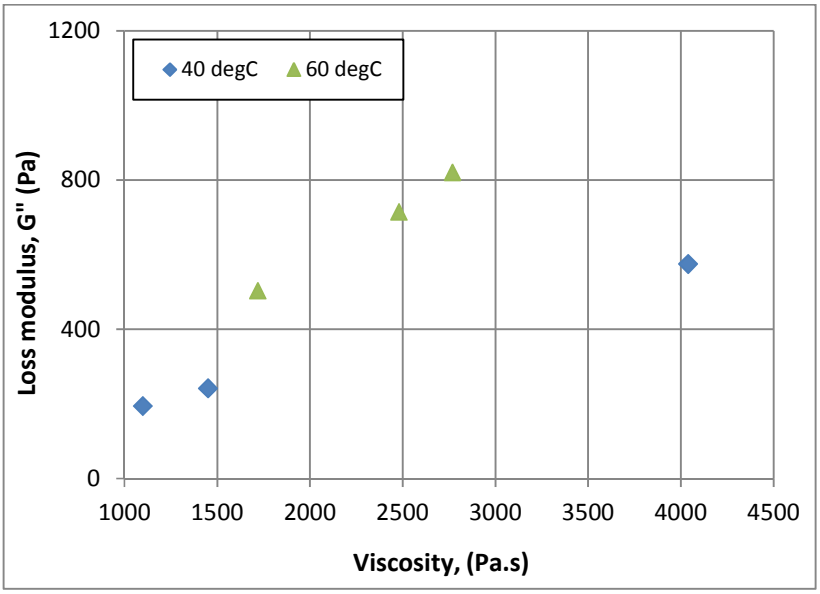

Figure 5.20. Viscosity vs. loss modulus of formed gel in the presence of ion Mg^{2+}.

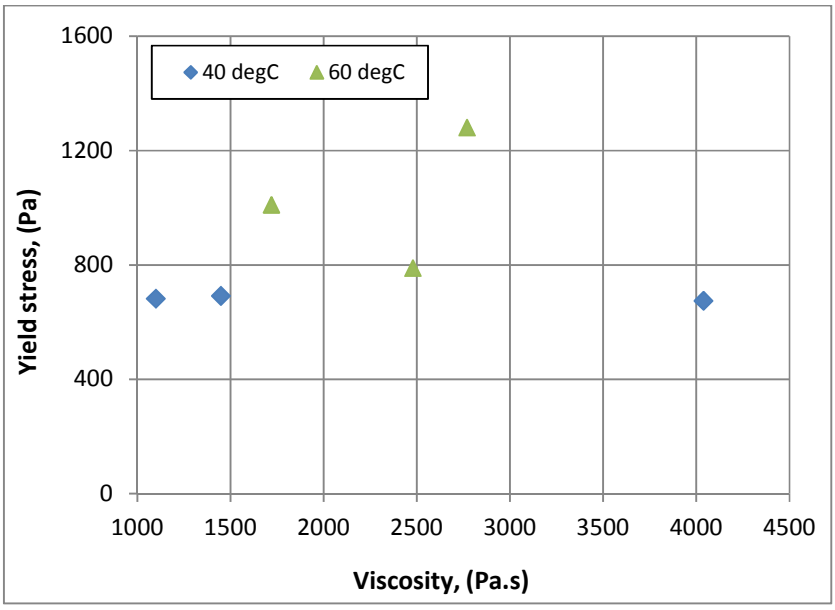

Figure 5.21. Viscosity vs. yield stress of formed gel in the presence of ion Mg^{2+}.

All three Figures showed the similar behaviors, which have been observed in the samples with ion Ca^{2+}.

5.8 Dilution effect

The injected sodium silicate system will meet with injected water that exists in the formation and will be diluted. The dilution will reduce the concentration of two main components of the gel system, which are sodium silicate solution and activator, thus will affect the sol-gel transition time.

In this section, experiments will be carried in a way to stimulate this situation, in which the injected gel system (sodium silicate solution and activator) will be mixed with distilled water in increased manner of quantity.

Gel preparation

In all samples, the quantities of sodium silicate solution (24 g) and activator (6 g) were kept constant. Distilled water was then added in each sample at amounts of 2.5 g, 5 g and 7.5 g.

The procedure of preparing samples is the same as in previous experiments.

Temperature setting

Four samples were tested at temperature 40^{o}C. Only two samples were tested at 50^{o}C and 60^{o}C. The temperatures are set in the same way as described in section 5.6.

Test procedure

All the samples were tested in 2 modes as described in section 5.2.

Test results and discussion

a. <u>Sol-gel transition time</u>

Experiment results are presented in Table 5.14 and sol-gel transition time is plotted vs. activator weight concentration in Figure 5.22.

Table 5.14. Sol-gel transition time at different dilution degree.

T, (°C)	Sample	Total sample weight (g)	Sodium silicate solution (wt%)	Activator (wt%)	DW (wt%)	Sol-gel transition time (hrs)	G' & G" at gel point (Pa)	Viscosity at gel point (Pa.s)
40	1	30	80.00%	20.00%	**0.00%**	**2.69**	0.60519	4.2786
	2	32.5	73.85%	18.46%	**7.69%**	**5.09**	0.52578	3.7176
	3	35	68.57%	17.14%	**14.29%**	**8.96**	0.48434	3.4248
	4	37.5	64.00%	16.00%	**20.00%**	**15.75**	0.43516	3.077
50	1	30	80.00%	20.00%	**0.00%**	**1.50**	0.57575	4.0663
	2	32.5	73.85%	18.46%	**7.69%**	**2.68**	0.46465	3.2844
60	1	30	80.00%	20.00%	**0.00%**	**0.89**	0.57555	4.0515
	2	32.5	73.85%	18.46%	**7.69%**	**1.43**	0.42001	2.9644

The results from Table 5.14 show that dilution has strong effect on sol-gel transition time. Every time 2.5 g of distilled water was added to the gel system, it made the sol-gel transition time longer almost 2 times.

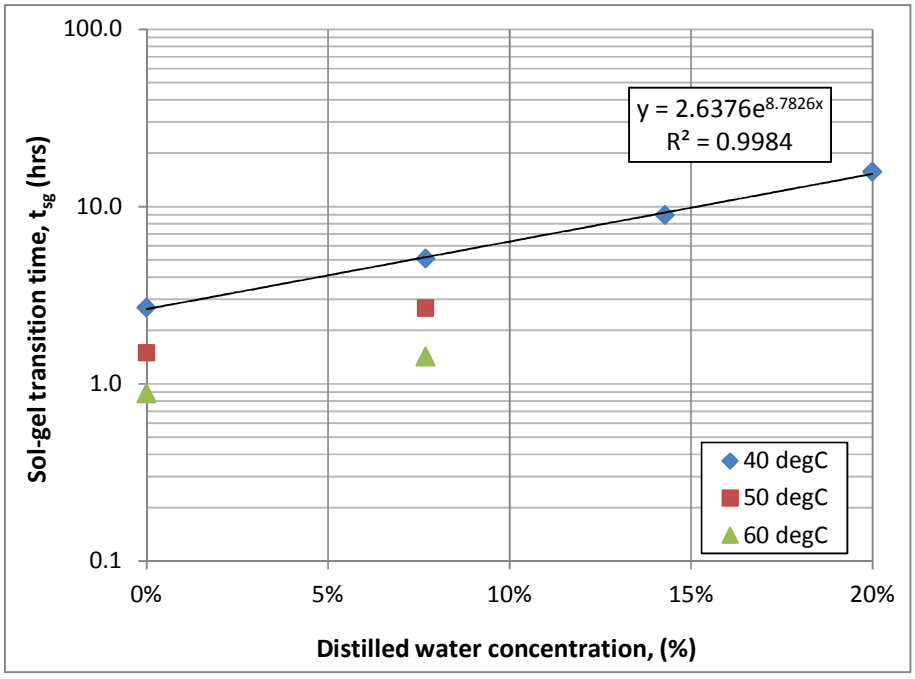

Figure 5.22. Effect of system dilution on sol-gel transition time.

The relation between sol-gel transition time and concentration of distilled water in the sample at 40°C is best described by the exponential function as follows:

$$t_{sg} = 2.6376 \times e^{8.7826[DW]}.$$

However, this function will not be used to build the unified sol-gel transition time correlation. The dilution effect will be expressed by the reduction in concentrations of two main components, sodium silicate solution and activator. The experiment results in this section will be used to check how accurate the estimation of sol-gel transition time under dilution effect.

b. Viscoelastic properties of formed gels

Table 5.15 presents values of limiting value of LVE range, yield stress, storage modulus and loss modulus of all samples at their tested viscosity values.

Table 5.15. Viscoelastic properties of the formed gel under dilution effect.

T, (°C)	Sample	DW (wt%)	Viscosity @ start of AS test (Pa.s)	Limiting value of LVE range (%)	Yield stress (Pa)	G' within LVE range (Pa)	G" within LVE range (Pa)
40	1	0.00%	108	6.23	70.4	1129	33.3
	2	7.69%	4040	1.64	674	40694	575.2
	3	14.29%	1100	5.19	580	11067	160.8
	4	20.00%	58	4.48	27	612.3	13.7
50	1	0.00%	5550	1.78	993	55655	1187.1
	2	7.69%	1210	2	246	12221	275.8
60	1	0.00%	8800	1.09	960	88491	2315.8
	2	7.69%	1720	4.79	868	17605	503.1

5.9 Derivation and verification of unified sol-gel transition time correlation

All derived functions between sol-gel transition time and different factors, which are studied in this work, are found and listed in Table 5.16.

Table 5.16. Summarization of all equations.

N^o	Factors	Equation
1	Activator	$t_{sg} = 1.3666 \times 10^{-3} \cdot [Ac]^{-4.7045}$
2	Sodium silicate solution	$t_{sg} = 8.4029 \times [SS]^{-3.5437}$
3	Temperature	$t_{sg} = 2.5432 \times 10^{-9} \times e^{\frac{6711.1}{T_K}}$
4	Ca^{2+} ion	$t_{sg} = 5.1119 \times e^{-0.007[Ca^{2+}]}$
5	Mg^{2+} ion	$t_{sg} = -0.0517 \times [Mg^{2+}] + 5.194$

The unified sol-gel transition time correlation is the combination of all five equations above. The matching coefficient $A = 5.9717 \times 10^{-4}$ is found based on various attempts to match the unified sol-gel transition time correlation with the conducted experiments results at different temperatures. However, it is noted that at high concentrations of divalent ions, above 1000 ppm in distilled water for Ca^{2+} and 500 ppm for Mg^{2+} and at temperature 60^{o}C, the general equation gives a large deviation from the experiment data. For example, 7.2% is difference between experimental and predicted values at concentration of 1000 ppm Ca^{2+} at 60^{o}C. The difference increased to 36.6% at the same Mg^{2+} concentration and at the same temperature. The reason for this large deviation could be explained by the precipitation, which starts to occur in the presence of high concentrations of divalent ions.

The unified sol-gel transition time correlation is written in the final form as follows:

$$t_{sg} = 5.9717 \times 10^{-4} \times [Ac]^{-4.7045} \times [SS]^{-3.5437} \times 10^{-9} \times e^{\frac{6711.1}{T_K}} \times e^{-0.007[Ca^{2+}]} \times (-0.0517 \times [Mg^{2+}] + 5.194).$$

Using this equation, the sol-gel transition time can be estimated from a given gel solution's composition and at a given reservoir condition (concentration of divalent ion Ca^{2+} and Mg^{2+}; reservoir temperature).

However, additional multiplication coefficients are needed to add to the unified sol-gel transition time correlation in the dilution cases to match the experiment data with predicted values. Since in the dilution cases, the total weight of gel system increased, the ratio between gel system weight before dilution and gel system weight after dilution need to be included into the unified sol-gel transition time correlation. In the Dilution effect section, four cases were studied with added water increased from 0 to 7.5 g (2.5 g of distilled water was added each time) to the gel system with original total weight 30 g (24 g of sodium silicate solution and 6 g of activator). So then the additional coefficient are calculated and listed in the Table below.

Table 5.17. Additional multiplication coefficients for dilution cases.

Sample	Total sample weight (g)	Additional multiplication coefficient
1	30	1
2	32.5	0.92
3	35	0.86
4	37.5	0.8

Additional experiments were conducted to test and verify the derived unified sol-gel transition time correlation both within and outside of its temperature range 40°C to 60°C. The composition of samples, test temperature and measured sol-gel transition results are presented in Table 5.18.

Table 5.18. Experiments for verification of derived unified sol-gel transition time correlation.

Sample	Total sample weight (g)	Activator (%)	Sodium silicate solution (%)	DW (%)	Ca^{2+}, (ppm)	Mg^{2+}, (ppm)	Test temperature		Sol-gel transition time, (hrs)		Difference (%)
							°C	°K	Calculated	Measured	
1	30	25%	68%	7%	0	0	35	308.15	2.38	2.21	7.2%
2		18%	75%	7%	0	0	45	318.15	3.97	4.01	1.0%
3		18%	75%	7%	0	0	55	328.15	2.09	1.98	5.0%
4		19%	74%	7%	0	0	55	328.15	1.70	1.66	2.5%
5		14%	79%	7%	0	0	65	338.15	3.09	2.25	27.3%
6		14%	79%	7%	0	0	70	343.15	2.32	1.66	28.4%
7	32.5	18.5%	73.8%	7.7%	11.54	11.54	40	313.15	4.27	4.17	2.3%
8		0.0%	0.0%	7.7%	23.08	9.23	50	323.15	4.21	4.11	2.4%

The tests on sample 7, 8 and 9 were performed to test the unified sol-gel transition time correlation when both of the divalent ions Ca^{2+} and Mg^{2+} exist in the sample simultaneously.

The sol-gel transition time from first five experiments are plotted in the same graph with the curves, which are generated from unified sol-gel transition time correlation at temperatures 35°C, 40°C, 45°C, 50°C, 55°C, 60°C and 65°C.

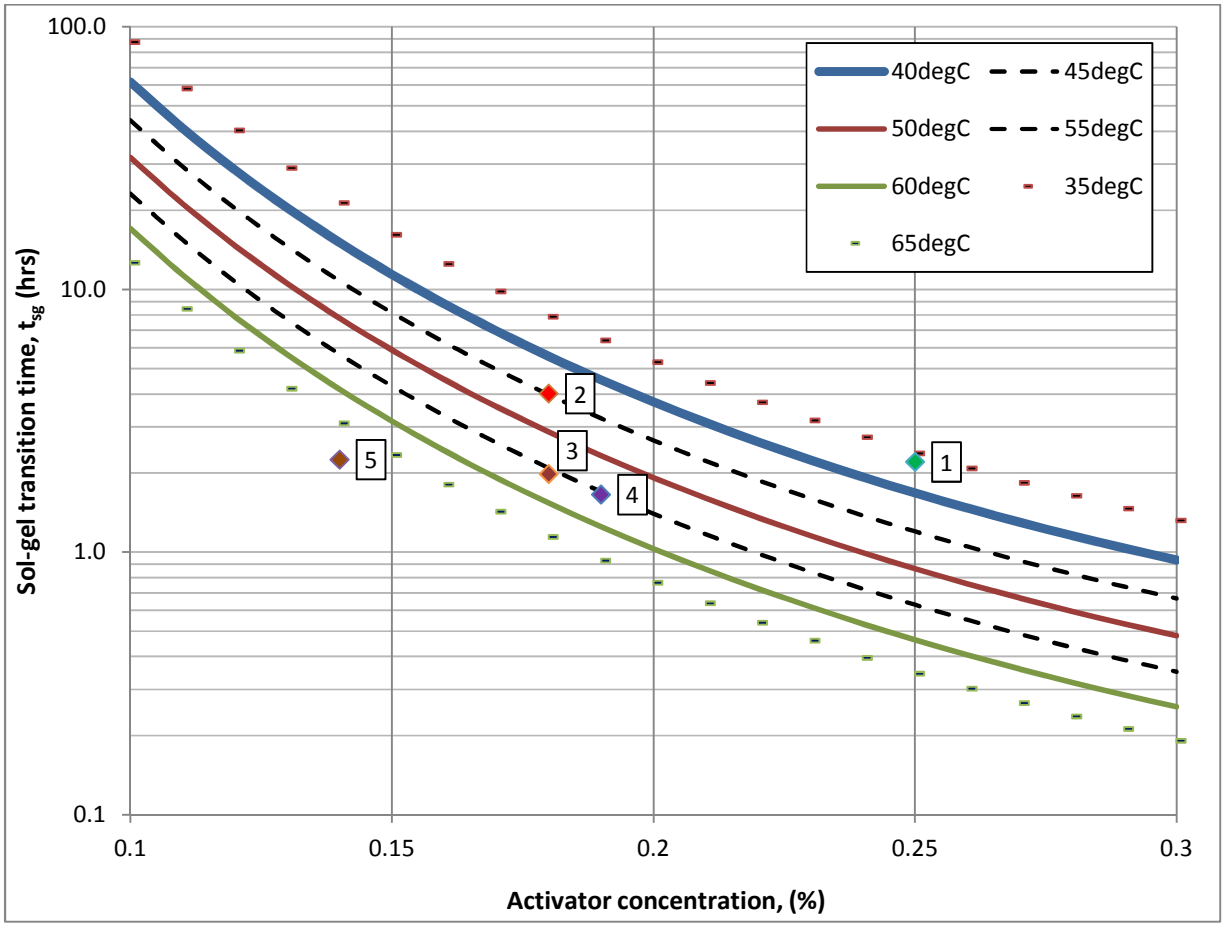

Figure 5.23. Verification of the unified sol-gel transition time correlation.

The test points within the temperature range of 40°C to 60°C (points 2, 3 and 4) show a good agreement with the predicted values (dashed lines). Extrapolation of the unified sol-gel transition time correlation outside the development temperate range (points 1 and 5) yields higher errors against measured experimental values.

The test points 7 and 8 with the presence of both divalent ions Ca^{2+} and Mg^{2+} also show a good agreement with predicted values.

5.10 Maximum differential pressure the formed gel can withstand

The yield stress of formed gels was obtained from second test mode and is in the relation with gel viscosity at testing time.

One example of calculation is presented in this section, which demonstrates how the maximum differential pressure is estimated from the yield stress of sample with composition of 14% activator (the rest is sodium silicate solution), by treating a natural fracture as a set of two parallel, smooth and impermeable planes. Figure 5.24 represents the Amplitude sweep test on this sample at viscosity equals 828 $Pa \cdot s$.

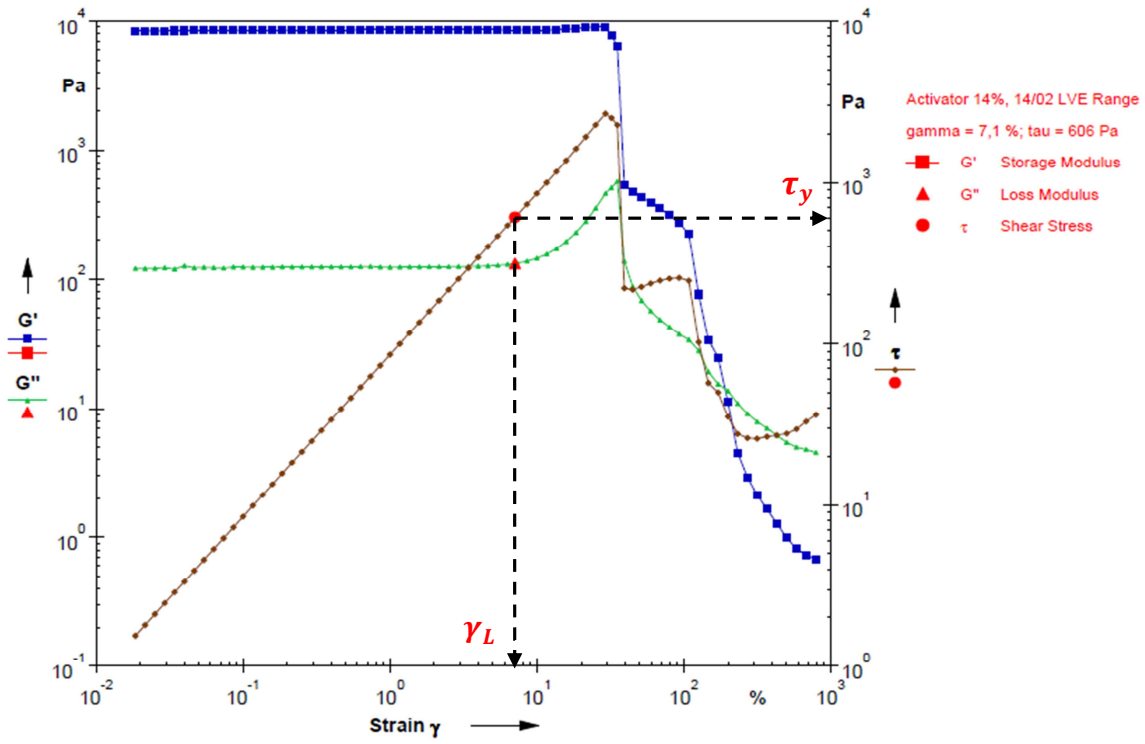

Figure 5.24. Amplitude sweep on sample with 14% of activator.

Test analysis based on measured date gives the result of yield stress equals 605 Pa (as shown in Figure 5.24).

One example of maximum differential pressure calculation at an effective distance of formed gel L = 20 m and a fracture width w = 0. 02 m is given below:

$$dP_{max} = \frac{2\tau_y}{w} dL = \frac{2 \cdot 606}{0.02} \cdot 20 = 12.12 \cdot 10^5\ Pa = 12.12\ bar.$$

In this work, the maximum differential pressures are estimated for a single fracture, which connects between injection and production well, at different fracture widths, *w*, vary from 1mm to 5 cm and effective distances of formed gel in the fracture L = 20, 50 and 100 m. The results are plotted in Figure 5.25.

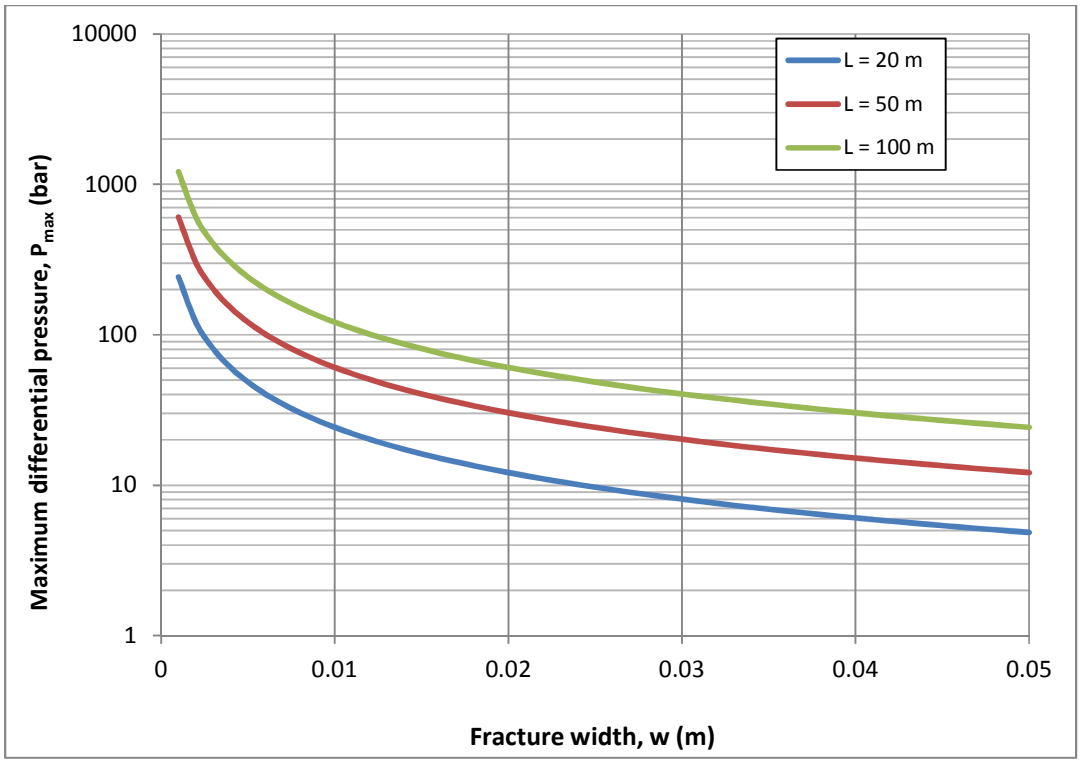

Figure 5.25. Maximum differential pressure the formed gel (14% of activator) can withstand at different fracture widths and effective distance from injection well.

Figure 5.25 shows an inverse relation between maximum differential pressure and fracture width; the smaller the fracture width, the higher maximum differential pressure the formed gel can withstand or in other words, a larger pressure gradient is needed for gel extrusion.

At the same fracture width, the longer the effective distance, the more difficult is the gel extrusion, since the formed gel now can withstand higher differential pressure.

Liu et al. (2001) have reported in their work that the calculated pressure gradient, Equation 3.14 greatly underestimates the pressure gradient required for gel extrusion through fractures in core flooding experiments. The reasons are:

- Macosko (1994) mentioned that for viscoelastic materials, wall-slip effects were particularly prevalent during yield stress measurement. Because of the impermeability of the wall, the layer of particles adjacent to the rheometer wall was typically more dilute than the bulk dispersion. During flow, the shear rate gradient caused particles to migrate away from the wall. The thin, dilute layer near the wall had a much lower viscosity – creating the impression that the bulk fluid was slipping along the wall. Since the yield point was a flow/no-flow as well as a transition point from elastic solid to viscous liquid, the existing thin, dilute layer acted as if the yield point had been reached and the material had already started to flow (Wang, et al., 2006). The measured yield stress, in this case, was lower than its actual value.
- Gels propagate through fractures by worm-holing through immobile concentrated (dehydrated) gel. Since these wormholes are narrower than the fracture width, this could partly explain the higher pressure gradient during the gel extrusion experiments (Wang, et al., 2006).
- In difference with smooth surface of measuring equipment, inherent presence of fracture wall surface heterogeneities (non-smooth surface) and the existence of small secondary fractures and/or wormholes in the core sample may increase significantly the differential pressure, which was estimated based on the above simple approach.

For this work, the calculation was just a demonstration to show the relationship between gel rheological properties (yield stress) and fracture properties (width and effective distance). It helps to predict the relative increase of maximum differential pressure, which the formed gel can withstand when the shut-in time is carried for longer time, since for a longer time, the viscosity of formed gel will be higher, thus earns the higher yield stress. However as mention in previous section, in some cases when the viscosity was too high, gel became more brittle and actually has lower limiting value of LVE range and also lower yield stress than the gel with lower viscosity.

6 Conclusions and Recommendations

Based on the observations from the experiments conducted during this study, the following conclusions can be made:

1. The gelation kinetics of silicate gel system is controlled by the concentration of silicate, the concentration of activator as well as temperature and presence of divalent ions (Ca^{2+} and Mg^{2+}).
    - The higher the concentration of activator in the gel system, the faster the gelation process, which leads to shorter sol-gel transition time.
    - Higher concentration of sodium silicate also tends to shorten the sol-gel gelation time, but at a lower intensity compared with the activator one.
    - Temperature has a significant effect on the gelation process – the higher the temperature, the shorter the sol-gel transition time and the faster the gelation rate. The relation between sol-gel transition time and temperature can be described using the Arrhenius equation.
    - The presence of divalent ions (Ca^{2+}, Mg^{2+}) also makes the sol-gel transition time shorter. Mg^{2+} ion has a higher potential for precipitation than Ca^{2+}. Concentration of 500 ppm Mg^{2+} in the makeup water (distilled water) caused precipitation, while a concentration of 1000 ppm of Ca^{2+} in makeup water resulted only to a more opaque gel solution.
    - Separate equations of sol-gel transition time were developed in relation to each one of these factors (sodium silicate concentration, activator concentration, temperature, divalent ion concentration (Ca^{2+}, Mg^{2+})), and a single unified sol-gel transition time correlation a function of all variables was derived by combining all separate equations along with a matching coefficient. This matching coefficient was found based on various attempts to fit the experiments results with unified sol-gel transition time correlation.
    - Dilution of the sodium silicate system will reduce the concentration of both sodium silicate and activator, thus increase the sol-gel transition time.
2. The general equation did not result into a very good match between the estimated and measured values when there is high concentration of divalent ion (starts from 1000 ppm for

Ca^{2+} and 500 ppm for Mg^{2+}) and at high temperature ($60^{o}C$). This could be due to the precipitation caused by the divalent ions at this high concentration.

3. Results from test experiments show a good estimation from unified sol-gel transition time correlation in the temperature range of $40^{o}C$ to $60^{o}C$ since the function of temperature effect was built based on experiments in this range.
4. The storage modulus G' of a formed gel is in direct proportion with viscosity, regardless the temperature, while the loss modulus G" is in direct proportion with viscosity and also the temperature.
5. In general, the yield stress is in directly proportion with viscosity except for a few experiments in which results were out of trend. The causes could come from measurement itself or from analysis program. Despite that fact, it was noticeable that at very high viscosities, the formed gel became brittle and was capable of withstanding a large deformation, thus leading to a low limiting value of LVE range and a low yield stress value.
6. The viscosity growth of a silicate gel system appears to behave differently from a polymer system. The viscosity growth of silicate gel follows the sequence of: a very low viscosity trend for a certain time period (prior to sol-gel transition time); a sharp increase after the sol-gel transition time; an increased growth rate until reaching a constant rate (constant slope on viscosity curve); and a slight decrease of the viscosity growth rate.
7. The gel strength of formed gel was evaluated by calculating the maximum differential pressure the formed gel can withstand, which is derived based on the minimum pressure gradient required to extrude the formed gel through two smooth parallel plates at a given yield stress. However, this approach greatly underestimates the pressure gradient required for gel extrusion through fractures in core flooding experiments or field conditions due to:
    - Wall-slip effects from equipment, which results in lower measured yield stress.
    - Gels propagate through fractures by worm-holing through immobile concentrated (dehydrated) gel and these wormholes are narrower than the fracture width.
    - Inherent presence of fracture wall surface heterogeneities (non-smooth surface) and the existence of small secondary fractures and/or wormholes in the core sample.

Recommendations for further works would be:

- Besides Ca^{2+} and Mg^{2+} ions, other divalent ions in the injected and formation water such as Ba^{2+}, Mn^{2+}, SO_4^{2-}, etc. will also affect the gel kinetics. The derived unified sol-gel transition time correlation will then include the effect of those divalent ions and give better estimation.
- Conduct experiments outside the temperature range of 40°C to 60°C, so that the function of temperature effect can be rebuilt, which will lead to better estimation from unified sol-gel transition time correlation in the wider range of temperature.
- Perform core flooding experiments on core samples to develop a correlation between calculated and measured values of maximum differential pressure the formed gel can withstand.

APPENDICES

Appendix A: Conversion between raw data (deflection angle φ) and rheological parameter (shear deformation γ) for concentric cylinder measuring system (CCMS) (Mezger, 2011).

$$\gamma = (60[s/min] \cdot C_{sr} \cdot \varphi)/2\pi = 9.55[s/min] \cdot C_{sr} \cdot \varphi \quad \text{(A.1)}$$

where C_{sr} – factor is the same for all ISO cylinder MS, independent of the radii of bob and cup since it always show the value C_{sr} = 1.291 min/s.

Appendix B: Relation between yield stress and maximum yield stress and maximum pressure drop in a fracture and in a porous matrix (Bird, et al., 1983).

The gel is assumed to behave like a Bingham fluid. The relation between the shear stress and the velocity gradient (or shear rate) in a shear flow $v_x = v_x(y)$ is (x is the flow direction and y the perpendicular to the shearing plane):

$$\begin{array}{ll} \tau_{yx} = \tau_0 + \eta_B \frac{dv_x}{dy} & \tau_{yx} > \tau_0 \\ \frac{dv_x}{dy} = 0 & \tau_{yx} < \tau_0 \end{array} , \quad \text{(B.1)}$$

where τ_0 is the yield stress and η_B the Bingham (or plastic) viscosity.

Under stationary (steady rate) conditions, the equation of motion is:

$$\nabla P + \nabla \cdot \tau = 0 \quad \text{(B.2)}$$

where p is the pressure field and τ is the stress tensor.

The fracture is modeled by two parallel plates of length L separated by a distance w (fracture width). The location of both plates is given by $y = \pm w/2$. Then, projecting the (vectorial) equation (2) onto the flow and pressure gradient direction x:

$$\nabla P + \frac{d}{dy}\tau_{yx} = 0 \quad \text{(B.3)}$$

i.e.,

$$\tau_{yx} = -\nabla P \cdot y + C \quad \text{(B.4)},$$

where the integration constant C is zero because of the symmetry of the problem. This equation clearly shows that the shear stress is maximum at the wall:

$$\tau_{wall} = \pm w\,\nabla P/2 \tag{B.5}$$

Therefore the Bingham fluid will withstand pressure gradients that do not exceed the value $2\tau_0/w$.

REFERENCES

Al-Anzi M.S., Al-Mutairi S.H. and Al-Khaldi M.H. Laboratory Evaluation of Organic Water Shut-off Gelling System for Carbonate Formations [Conference] // SPE European Formation Damage Conference. - Noordwijk, The Netherlands : SPE, 2011.

Bailey B. [et al.] Water Control [Article] // Oilfield review. - 2000. - p. 30.

Bedaiwi E. [et al.] Polymer Injection for Water Production Control through Permeability Alteration in Fractured Reservoir [Article] // NAFTA. - 2009. - 4 : Vol. 60.

Beecroft W.H., Maier, L.F. [Patent] : Patent 808312. - US, 1969.

Bird R.B. and Dai. G.C. Yarusso B.J. The Rheology and Flow of Viscoplastic Materials [Article] // Reviews in Chemical Enginering. - 1983. - 1 : Vol. 1.

Bjørn B. [et al.] Development and Evaluation of a New Environmentally Acceptable Conformance Sealant [Conference] // SPE European Formation Damage Conference. - Noordwijk, The Netherlands : SPE, 2011.

Bol G.M. [et al.] The Development of a Silicate-based Drilling Fluid [Book Section] // Chemical in the Oil Industry, Recent Development . - [s.l.] : Royal Society of Chemistry, 1998.

Bowers B. E., Brownlee R. F. and Schrenkel P.J. Develoopment of a Dowhole Oilwater Separation and Reinjection System for Offshore Application [Conference] // Offshore Technology Conference. - [s.l.] : SPE 8865-MS, 1998.

Callister W.D. Jr. Materials Science and Engineering, An Introduction, fouth edition [Book Section]. - New York : John Wiley & Sons Inc., 1997.

Iler R.K. The Chemistry of Silica, Solubility, Polymerization, Colloid and Surface Properties, and Biochemistry [Book]. - [s.l.] : Wiley-Interscience, 1979.

Karmakar G.P. and Chakraborty C. Improved oil recovery using polymeric gelants: A review [Article] // Indian Journal of Chemical Technology. - 2006. - Vol. 13.

Krumrine P.H. and Boyce S.D. Profile Modification and Water Control With Silica Gel-Based Systems [Conference] // International Symposium on Oilfield and Geothermal Chemistry. - Phoenix : SPE 13578-MS, 1985.

Lakatos I. [et al.] Application of Silicate-Based Well Treatment Techniques at the Hungarian Oil Fields [Conference] // SPE Annual Technical Conference and Exhibition. - Houston, Texas : SPE 56739-MS, 1999.

Lakatos I., Lakatos-Szabo J. and Miskolc-Egyetemvaros Reservoir Conformance Control in Oilfield Using Silicates: State-of-the-Arts and Perspectives [Conference] // SPE Anual Technical Conference and Exhibition . - San Antonio, USA : SPE 159640, 2012.

Liu J. and Seright R.S. Rheology of Gels Used for Conformance Control in Fractures [Conference] // SPE/DOE Improved Oil Recovery Symposium. - Tulsa, Oklahoma : SPE, 2001.

Macosko C.W. Rheology Principles, Measurements and Applications [Book Section]. - New York : WILEY - VCH, 1994.

Macosko C.W. Rheology Principles, Measurements, and Applications [Book]. - New York City : WILEY-VCH, 1994. - pp. 97-98, 108-140.

Mezger T.G. The Rheology Handbook [Book]. - Hanover : Vincentz Network, 2011.

Nasr-El-Din H.A. and Taylor K.C. Evaluation of sodium silicate/urea gels used for water shut-off treatments [Article] // Journal of Petroleum Science and Engineering. - [s.l.] : Elsevier, 2005. - 3-4 : Vol. 48.

Perez D., Fragachan, F.E, Ramirez A. and Ferraud J.P. Application of polymer gel for establishing zonal isolation and water shutoff in carbonate formation [Article] // SPE Drilling & Completion. - [s.l.] : SPE, 1997. - 3 : Vol. 16.

Portwood J. Lessons Learned from Over 300 Producing Well Water Shut-off Gel Treaments [Conference] // SPE Mid-Continent Operations Symposium. - Oklahoma : SPE 52127, 1999. - doi:10.2118/52127-MS.

Schiozer D.J. and Paulo J. Methodology to Compare Smart and Conventional Wells [Conference] // SPE Annual Technical Conference and Exhibition. - New Orleans, Louisiana, U.S.A : SPE 124949, 2009.

Schlumberger Intelligent completions [Journal]. - [s.l.] : Schlumberger, 2001. - 2, pages 24-43 : Vol. 8.

Skrettingland K., Giske N.H. and Johnsen J., Stavland, A. Snorre In-depth Water Diversion Using Sodium Silicate - Single Well Injection Pilot [Conference] // SPE Improved Oil Recovery Symposium 18th. - Tulsa, OK, USA : SPE 154004, 2012.

Stavland A. [et al.] In-depth Water Diversion Using Sodium Silicate – Preparation for Single Well Field Pilot on Snorre [Conference] // 16th European Symposium on Improved Oil Recovery. - Cambridge, UK : [s.n.], 2011.

Sydansk R.D. A Newly Developed Chromium(lll) Gel Technology [Conference] // SPE Reservoir Engineering. - [s.l.] : SPE, 1990.

Vafaie Sefti M. [et al.] Polyacrylamide Gel Polymer as Water Shut-off System: Preparation and Investigation of Physical and Chemical Properties in One of the Iranian Oil Reservoirs Conditions [Journal]. - [s.l.] : Iranian Journal of Chemistry & Chemical Engineering, 2007. - 4 : Vol. 26.

Vinot B., Schechter R.S. and Lake L.W. Formation of Water-Soluble Silicate Gels by the Hydrolysis of a Diester of Dicarboxylic Acid Solublized as Microemulsions [Journal]. - [s.l.] : Society of Petroleum Engineers, 1989. - Vols. Volume 4, Number 3.

Wang Y. and Seright R.S. Correlating Gel Rheology With Behavior During Extrusion Through Fractures [Conference] // SPE/DOE Symposium on Improved Oil Recovery. - Tulsa, Oklahoma : SPE 99462, 2006.

Wu G., Reynolds K. and Markitell B. A Field Study of Horizontal Well Design in Reducing Water Coning [Conference] // International Meeting on Petroleum Engineering. - Beijing, China : SPE, 1995.